Third edition

Theory of Plasticity

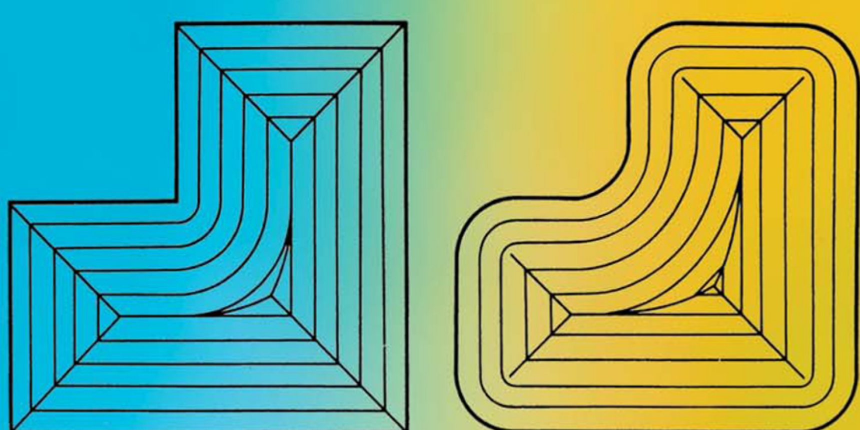

J. Chakrabarty

THEORY OF PLASTICITY

To my wife, Swati

THEORY OF PLASTICITY

Third edition

J. Chakrabarty

Formerly, Professor of Mechanical Engineering,
Texas A & M University System, USA

ELSEVIER

AMSTERDAM • BOSTON • HEIDELBERG • LONDON • NEW YORK • OXFORD
PARIS • SAN DIEGO • SAN FRANCISCO • SINGAPORE • SYDNEY • TOKYO
Butterworth-Heinemann is an imprint of Elsevier

Butterworth-Heinemann is an imprint of Elsevier
Linacre House, Jordan Hill, Oxford OX2 8DP
30 Corporate Drive, Suite 400, Burlington, MA 01803

First published by McGraw-Hill Inc. 1987
Second edition 1998
Third edition published by Elsevier Butterworth-Heinemann 2006

British Library Cataloguing in Publication Data
A catalogue record for this book is available from the British Library

Library of Congress Cataloging-in-Publication Data
A catalog record for this book is available from the Library of Congress

ISBN-13: 978-0-7506-6638-2
ISBN-10: 0-7506-6638-2

For information on all Butterworth-Heinemann publications
visit our web site at http://books.elsevier.com

Printed and bound in the UK

06 07 08 09 10   10 9 8 7 6 5 4 3 2 1

CONTENTS

ABOUT THE AUTHOR

Professor J. Chakrabarty received his Ph.D. in Mechanical Engineering in 1966 from the Imperial College of Science and Technology, London, under the supervision of Professor J. M. Alexander. After spending a couple of years at the Middle East Technical University, Ankara, as an Assistant Professor, he accepted a faculty position at the University of Birmingham, England, where he remained till 1980. He subsequently moved to the United States as a Professor of Mechanical Engineering at the University of Utah. Professor Chakrabarty has made important contributions in the area of plasticity through the publication of numerous papers in professional journals of international reputation.

PREFACE TO THE THIRD EDITION

Since its first publication, *Theory of Plasticity* has been well received by both students and instructors across the world, and has been generally recognized as a useful exposition of the mechanics of plastic deformation of metals. The many encouraging comments I have received over the years from professors and researchers in the field of plasticity have prompted me to prepare a revised third edition of the book. Although several other works on plasticity have appeared since the first publication of this book, there is apparently none that deals with the specific areas of application treated in this book with comparable degrees of completeness.

The major addition to this third edition consists of the addition of a new Chapter 9 that deals with numerical methods of solving elastic/plastic problems, using both the finite difference and finite element methods. A new section has been added to Chapter 4 to discuss the limit analysis of space frames, including grillages, which involve beams under combined loading. A number of recent references to the published literature on plasticity are made in appropriate footnotes throughout the book. A set of new homework problems is also included at the end of several chapters for the benefit of both the student and the instructor, and worked solutions for instructors are provided on the accompanying website at http://textbooks.elsevier.com.

It is hoped that this new edition will continue to be useful for teaching and research in the field of plasticity. Though intended primarily for graduate students, there is also material in the book that could be used for senior undergraduate students and by practicing engineers. The book will also serve as a suitable reference work for numerous other courses related to solid mechanics.

I would like to express my sincere gratitude to Professor J. M. Alexander, who has always encouraged me with his admiration for this work. I am also grateful to Professor W. Johnson for his support. It is a great pleasure to express my sincere thanks to Mr. J. Simpson of Elsevier for his unfailing support and cooperation in bringing out the revised third edition of the book. Above all, I am profoundly grateful to Ma Indira Devi, who graciously provided the inspiration that was so necessary for the satisfactory completion of this work.

J. Chakrabarty

This page intentionally left blank

PREFACE TO THE FIRST EDITION

During recent years, there has been considerable interest in the application of the macroscopic theory of plasticity to engineering problems associated with structural designs and the technological forming of metals. The need for a comprehensive text book on plasticity, incorporating the most recent developments of the subject, has been strongly felt for some years. This book has been written primarily to meet the needs of graduate and research students of Mechanical, Civil, and Metallurgical Engineering, although some of the material in the book is also suitable for undergraduate students and practicing engineers. In order to discuss the various topics as fully as possible, it has been found necessary to treat the subject matter in two volumes, of which the first one is now presented to the reader.

The first chapter of the book deals with the analysis of stress and strain rate, and introduces the definition of the stress rate. The second chapter discusses the yield criteria, stress–strain relations, uniqueness theorems, and extremum principles. A series of physical problems where elastic and plastic strains are simultaneously important are discussed in Chaps. 3 and 5. A detailed account of the limit analysis of framed structures is given in Chap. 4 as a logical continuation of the treatment of the bending of beams. The remaining chapters of the book deal with the theory and application of slipline fields, an area that has received the greatest attention in the literature. The basic theory is explained in Chap. 6, which includes the recent analytical and numerical methods of solution of the plane strain problem. A variety of practical problems involving steady, pseudosteady, and nonsteady states of plastic flow are thoroughly discussed in Chaps. 7 and 8. Several numerical tables are presented in the Appendix to facilitate the computation of slipline field solutions.

Tensor or suffix notation is introduced in the first chapter, where the summation convention and the associated algebraic operations have been explained for the benefit of those readers who are unfamiliar with them. The suffix notation is a convenient shorthand for writing the general equations, and is practically indispensable in the derivation of general theorems. Bessel functions are extensively used in the latter half of Chap. 6 for the analytical solution of boundary-value problems involving slipline fields. These sections may be omitted during the first reading, provided the results used in the subsequent chapters for the solution of special problems are taken for granted. I have made an earnest endeavor to make the treatment of each problem as complete as is warranted by the present state of knowledge. A large number of exercise problems are provided at the end of each chapter to enable the student to test his or her mastery of the subject. There is more material in this book than can be covered in a one-semester course on plasticity, so that the instructor has sufficient flexibility in the selection of topics.

References to original papers and books relating to plasticity and its applications have been given in numerous footnotes throughout the book. The literature in the field of plasticity is so extensive that I have been compelled to restrict myself mainly to publications that appeared in English. The reader would be able to form a list of publications in other languages from some of the references cited in this book. Although an exhaustive bibliography has not been attempted, I wish to express my sincere regrets for any inadvertent omission of important publications.

I would like to thank the following professors for reviewing the manuscript: David H. Allen, Texas A & M University; Nicholas J. Altiero, Michigan State University; James M. Gere, Stanford University; Kerry S. Havner, North Carolina State University; Philip G. Hodge, University of Minnesota; Francis T. C. Loo, Clarkson University; Huseyin Sehitoglu, University of Illinois; and David J. Unger, Ohio State University.

I take this opportunity to record my profound appreciation of the cooperation offered by the officers of McGraw-Hill Book Company during the planning and production of the book. I am indebted to Albert Harrison, Harley Editorial Services for his ready cooperation while dealing with the proofs.

J. Chakrabarty

CHAPTER

ONE

STRESSES AND STRAINS

1.1 Introduction

The theory of plasticity is the branch of mechanics that deals with the calculation of stresses and strains in a body, made of ductile material, permanently deformed by a set of applied forces. The theory is based on certain experimental observations on the macroscopic behavior of metals in uniform states of combined stresses. The observed results are then idealized into a mathematical formulation to describe the behavior of metals under complex stresses. Unlike elastic solids, in which the state of strain depends only on the final state of stress, the deformation that occurs in a plastic solid is determined by the complete history of the loading. The plasticity problem is, therefore, essentially incremental in nature, the final distortion of the solid being obtained as the sum total of the incremental distortions following the strain path.

A metal may be regarded as macroscopically homogeneous and isotropic when the small crystal grains forming the aggregate are distributed with random orientations. As a result of plastic deformation, the crystallographic directions gradually rotate toward a common axis, producing a *preferred orientation*. An initially isotropic material thereby becomes anisotropic, and its mechanical properties vary with direction. The development of anisotropy with progressive cold work and the resulting strain-hardening are too complex to be successfully incorporated in the theoretical framework. In the mathematical theory of plasticity, it is generally assumed that the material remains isotropic throughout the deformation irrespective of the degree of cold work. Since the strain-hardening characteristic of a metal in a complex state of stress can be related to that in uniaxial tension or compression, it is necessary to examine the uniaxial stress–strain behavior in some detail before considering the general theory of plasticity.

The plastic deformation in a single crystal is generally produced by slip, which is the sliding of adjacent blocks of the crystal along definite crystallographic planes, called slip planes. The boundary line separating the slipped region of a crystal from the neighboring unslipped region is called a *dislocation.* The movement of the dislocation, which is responsible for the slip, is initiated by a line defect causing a local concentration of stress. Slip usually occurs on those planes which are most densely packed with atoms. The magnitude and direction of the relative movement in a slip is specified by a vector known as the *Burgers vector*. A dislocation is said to be one of unit strength when the magnitude of the Burgers vector is equal to one atomic spacing. The terms *edge dislocation* and *screw dislocation* are used to describe the situations where the Burgers vector is normal and parallel respectively to the dislocation line. In general, a dislocation is partly edge and partly screw in character, and the dislocation line forms a curve or a closed loop.†

In a polycrystalline metal, the crystallographic orientation changes from one grain to the next through a narrow transition zone, or grain boundary, which acts as an effective barrier to slip. Dislocations pile up along the active slip planes at the grain boundaries, the effect of which is to oppose the generations of new dislocations. When the applied stress is increased to a critical value, the shear stress developed at the head of the dislocation pile-up becomes large enough to cause dislocation movement across the boundary. The dislocation pile-up is mainly responsible for strain-hardening of the metal in the early stages of plastic deformation. The rate of hardening of the polycrystalline metal is always higher than that of the single crystal, where the increase in yield stress is caused by dislocations interacting with one another and with foreign atoms serving as barriers. The dislocation interactions control the yield strength of a polycrystalline metal only in the later stages of the deformation.

If the temperature of the strain-hardened metal is progressively increased, the cold-worked state becomes more and more unstable, and the material eventually reverts to the unstrained state. The overall process of heat treatment that restores the ductility to the cold-worked metal is known as *annealing.* The temperature at which there is a marked decrease in hardness of the metal is known as the *recrystallization temperature*. The dislocation density decreases considerably on recrystallization, and the cold-worked structure is replaced by a set of new strain-free grains. The greater the degree of cold-work, the lower the temperature necessary for recrystallization, and smaller the resulting grain size.‡

In ductile metals, under favorable conditions, plastic deformation can continue to a very large extent without failure by fracture. Large plastic strains do occur

† For a complete discussion, see A. H. Cottrell, *Dislocations and Plastic Flow in Crystals*, Clarendon Press, Oxford (1953); W. T. Read, *Dislocations in Crystals*, McGraw-Hill Book Company, New York (1953); J. Friedel, *Dislocations*, Addison-Wesley Publishing Company, Reading, Mass. (1964); F. R. N. Nabarro, *Theory of Crystal Dislocations*, Clarendon Press, Oxford (1967); D. Hull, *Introduction to Dislocations*, 2d ed., Pergamon Press, Oxford (1975).

‡ See, for example, G. E. Dieter, *Mechanical Metallurgy*, Chap. 5, 2d ed., McGraw-Hill Book Company, New York (1976). See also R. W. K. Honeycombe, *The Plastic Deformation of Metals*, 2d ed., Edward Arnold, London (1984).

in many metal-working processes, which constitute an important area of application of the theory of plasticity. While elastic strains may be neglected in such problems, the continued change in geometry of the workpiece must be allowed for in the theoretical treatment. Severe plastic strains are produced locally in certain mechanical tests such as the hardness test and the notch tensile test. The significance of these tests cannot be fully appreciated without a knowledge of the extent of the plastic zone and the associated state of stress. Situations in which elastic and plastic strains are comparable in magnitude arise in a number of important structural problems when the loading is continued beyond the elastic limit. Structural designs based on the estimation of collapse loads are more economical than elastic designs, since the plastic method takes full advantage of the available ductility of the material.

1.2 The Stress–Strain Behavior

(i) ***The true stress–strain curve*** The stress–strain curve of an annealed material in simple tension is found to coincide with that in simple compression when the true stress σ is plotted against the true or natural strain ε. The *true stress*, defined as the load divided by the current cross-sectional area of the specimen, can be significantly different from the *nominal stress*, which is the load per unit original area of cross-section. Let l denote the current length of a tensile specimen and dl the increase in length produced by a small increment of the stress. Then the true strain increases by the amount $d\varepsilon = dl/l$. If the initial length is l_0, the total strain is $\varepsilon = \ln(l_0/l)$, called the true or *natural strain.*† For a specimen uniformly compressed from an initial height h_0 to a final height h, the magnitude of the natural strain is $\varepsilon = \ln(h_0/h)$. The conventional or *engineering strain e*, on the other hand, is the amount of extension or contraction per unit original length or height. It follows that $\varepsilon = \ln(l + e)$ in the case of tension, and $\varepsilon = -\ln(l - e)$ in the case of compression. Thus ε becomes progressively lower than e in tension, and higher than e in compression, as the deformation is continued in the plastic range.

Figure 1.1 shows the true stress–strain curve of a typical annealed material in simple tension. So long as the stress is sufficiently small, the material behaves elastically, and the original size of the specimen is regained on removal of the applied load. The initial part of the stress–strain curve is a straight line of slope E, which is known as Young's modulus. The point A represents the *proportional limit* at which the linear relationship between the stress and the strain ceases to hold. The elastic range generally extends slightly beyond the proportional limit. For most metals, the transition from elastic to plastic behavior is gradual, owing to successive yielding of the individual crystal grains. The location of the *yield point* B is, therefore, largely a matter of convention. The corresponding stress Y, known as the yield stress, is generally defined as that for which a specified small amount of permanent deformation is observed. For theoretical purposes, it is often convenient

† The concept of natural strain has been introduced by P. Ludwik, *Elemente der Technologischen Mechanik*, Springer Verlag, Berlin (1909). The natural strains associated with successive deformations are additive, but the engineering strains are not.

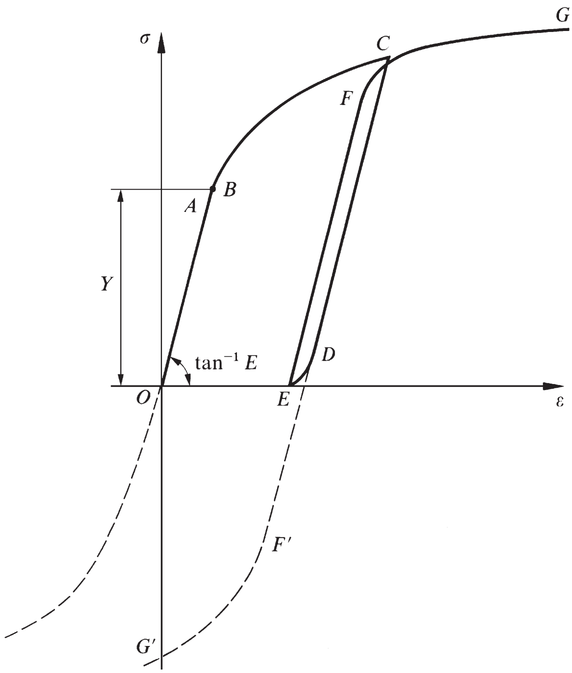

Figure 1.1 True stress–strain curve of metals with effects of unloading and reversed loading.

to assume a sharp yield point defined by the intersection of a pair of straight lines, one of which is a continuation of *OA* and the other a tangent to the stress–strain curve at a point slightly above *B*.

Beyond the yield point, the stress continually increases with further plastic strain, while the slope of the stress–strain curve, representing the rate of strain-hardening, steadily decreases with increasing stress. If the specimen is stressed to some point *C* in the plastic range and the load is subsequently released, there is an elastic recovery following the path *CD* which is very nearly a straight line† of slope *E*. The permanent strain that remains on complete unloading is equal to *OE*. On reapplication of the load, the specimen deforms elasticity until a new yield point *F* is reached. Neglecting the hysteresis loop of narrow width formed during the loading and unloading, *F* may be taken as coincident with *C*. On further loading, the stress–strain curve proceeds along *FG*, virtually as a continuation of the curve *BC*. The curve *EFG* may be regarded as the stress–strain curve of the metal when prestrained by the amount *OE*. The greater the degree of prestrain, the higher the new yield point and the flatter the strain-hardening curve. For a heavily prestrained metal, the rate of strain-hardening is so small that the material may be regarded as approximately nonhardening or *ideally plastic*.

A generic point on the stress–strain curve in the plastic range corresponds to a recoverable elastic strain equal to σ/E, and an irrecoverable plastic strain equal

† L. Prandtl, *Z. angew. Math. Mech.*, **8**: 85 (1928).

to $\varepsilon - \sigma/E$. If the stress is plotted against the plastic strain only, and the material is assumed to have a sharp yield point, the resulting curve will begin at $\sigma = Y$. Let H be the slope of the true stress–strain curve excluding the elastic strain, and T the slope of the curve including the elastic strain, for a given value of the stress σ. The quantities H and T are known as the *plastic modulus* and the *tangent modulus* respectively. A stress increment $d\sigma$ produces an elastic strain increment $d\sigma/E$ and a plastic strain increment $d\sigma/H$, while the total strain increment is $d\sigma/T$. Hence the relationship between H and T is

$$\frac{1}{T} = \frac{1}{E} + \frac{1}{H} \tag{1}$$

In an annealed material, H is considerably greater than T at the initial yielding, but these two moduli rapidly approach one another as the strain is increased. The difference between H and T becomes insignificant when the slope is only a few times the yield stress. At this stage, the elastic strain increment becomes negligible in comparison with the plastic strain increment. When the total strain is sufficiently large, the elastic strain itself is negligible. The stress–strain behavior at sufficiently large strains is identical to that of a hypothetical material in which E is infinitely large. Such a material is regarded as *rigid/plastic*, since it remains undeformed so long as the stress is below the yield point, while the subsequent deformation is entirely plastic.

Suppose that a specimen that has been completely unloaded from a tensile plastic state, represented by the point C, is reloaded in simple compression (Fig. 1.1). The stress–strain curve will then follow the path DF', where the new yield point F' corresponds to a stress that is appreciably smaller in magnitude than that at C. This phenomenon is known as the *Bauschinger effect*,† which occurs in real metals whenever there is a reversal of the stress. The subsequent strain-hardening follows the path $F'G'$, and approaches the stress–strain curve in compression as the loading is continued. The lowering of the yield stress in reversed loading is mainly caused by residual stresses that are left in the specimen on a microscopic scale due to the different stress states in the individual crystals. The Bauschinger effect can, therefore, be largely removed by a mild annealing. In the theory of plasticity, it is generally necessary to neglect the Bauschinger effect, the material being assumed to have identical yield stresses in tension and compression irrespective of the previous cold-work.

Some metals, such as annealed mild steel, exhibit a sharp yield point followed by a sudden drop in the stress, which remains approximately constant during a small amount of further straining. The sharp peak is known as the upper yield point, which is usually 10 to 20 percent higher than the lower yield point represented by the constant stress. At the upper yield point, a lamellar plastic zone, known as *Lüder's band*, inclined at approximately 45° to the tensile axis, appears at a local stress concentration. During the subsequent elongation under constant stress, several Lüder's bands appear and gradually spread over the entire specimen. After a total yield point elongation of about 10 percent, the stress begins to rise again due to

† J. Bauschinger, *Zivilingenieur*, **27**: 289 (1881).

strain-hardening, and the stress–strain curve then continues as before. The yield point drop is suppressed by a light cold-work, but the phenomenon reappears after the metal has been rested for several days at room temperature, or several hours at a relatively high temperature.†

(ii) ***Some consequences of work-hardening*** A longitudinal extension in the tensile test is accompanied by a contraction in the lateral direction. The ratio of the magnitude of the lateral strain increment to that of the longitudinal strain increment is known as the *contraction ratio*, denoted by η. In the elastic range of deformation, the contraction ratio has a constant value equal to Poisson's ratio ν. When the yield point is exceeded, the plastic part of the lateral strain increment for an isotropic material is numerically equal to one-half of the longitudinal plastic strain increment. Since the ratio of the elastic parts of the lateral and longitudinal strain increments is equal to $-\nu$, the total lateral strain increment in uniaxial tension is

$$d\varepsilon' = -\tfrac{1}{2}d\varepsilon + (\tfrac{1}{2} - \nu)d\varepsilon^e$$

where $d\varepsilon^e$ is the elastic part of the longitudinal strain increment $d\varepsilon$. In view of the relationship $d\varepsilon^e = d\sigma/E = (T/E)d\varepsilon$, the contraction ratio becomes

$$\eta = -\frac{d\varepsilon'}{d\varepsilon} = \tfrac{1}{2} - (\tfrac{1}{2} - \nu)\frac{T}{E} \tag{2}$$

Since the slope of the stress–strain curve decreases fairly rapidly in the early stages of strain-hardening, the contraction ratio rapidly approaches the asymptotic value of 0.5 as the strain is increased in the plastic range.‡ For a material having a sharp yield point, the contraction ratio changes discontinuously at this point to a value that depends on the initial rate of strain-hardening. When the tangent modulus becomes of the same order as that of the current yield stress, $\eta \simeq 0.5$, and the incremental change in volume becomes negligible.

The standard tensile test is unsuitable for obtaining the stress–strain curve of metals up to large values of the strain, since the specimen begins to neck when the rate of hardening decreases to a critical value. At this stage, the increase in load due to strain-hardening is exactly balanced by the decrease in load caused by the diminution of the area of cross section. Consequently, the load attains a maximum at the onset of necking. The longitudinal load at any stage is $P = \sigma A$, where A is the current cross-sectional area and σ the current stress, and the corresponding volume of the specimen is lA, where l is the current length. Using the constancy of volume, the maximum load condition $dP = 0$ may be written as

$$\frac{d\sigma}{\sigma} = -\frac{dA}{A} = \frac{dl}{l}$$

† In addition to low-carbon steel, yield point phenomenon has been observed in aluminum, molybdenum, and titanium alloys.

‡ For an experimental investigation on the variation of the contraction ratio, see A. Shelton, *J. Mech. Eng. Sci.*, **3**: 89 (1961).

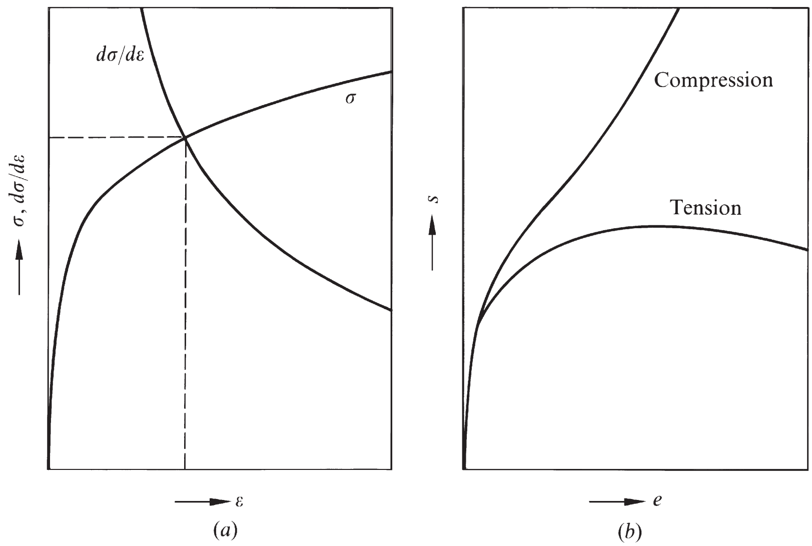

Figure 1.2 Peculiarities in tension and compression. (*a*) Location of point of tensile necking; (*b*) nominal stress versus engineering strain.

Since dl/l is equal to $d\varepsilon$, the condition for the onset of necking becomes

$$\frac{d\sigma}{d\varepsilon} = \sigma \tag{3}$$

When the true stress–strain curve is given, the point on the curve that corresponds to the tensile necking can be located graphically from the fact that the slope at this point is equal to the current stress (Fig. 1.2*a*). A heavily prestrained metal will obviously neck as soon as the yield point is exceeded. Since $d\varepsilon = de/(1+e)$, the condition for necking can be expressed in the alternative form

$$\frac{d\sigma}{de} = \frac{\sigma}{1+e}$$

It follows that the maximum load corresponds to the point of contact of the tangent to the (σ, e) curve from the point $(-1, 0)$ on the negative strain axis.† The tensile test becomes unstable when the load reaches its maximum. The deformation is confined locally in the neck, while the remainder of the specimen recovers elastically under decreasing load until fracture intervenes. The stress distribution in the neck assumes a triaxial state which varies through the cross section of the neck. The test no longer provides a direct measure of the stress–strain behavior. Although the stress–strain curve may be continued by introducing a correction factor that requires

† A Considere, *Ann. ponts et chausses*, **6**: 574 (1885). An interesting discussion has been given by C. R. Calladine, *Engineering Plasticity*, Chap. 2, Pergamon Press, Oxford (1969).

careful measurements of the geometry of the neck,† the experimental difficulties render the method unsuitable for practical purposes.‡

The strain-hardening characteristic of metals at large strains is most conveniently obtained by compressing a solid cylindrical specimen between a pair of parallel platens. In the absence of efficient lubrication, the compression test is complicated by the fact that the friction at the platens restricts the metal flow at the ends of the specimen, causing barreling as the compression proceeds. Since homogeneous compression is thus prevented by friction, the stress–strain curve cannot be derived by the direct measurement of the load and the change in height of the specimen. In actual practice, the difficulty is overcome by using several cylinders with different initial diameter/height ratios, subjecting them to the same load each time on an incremental basis, and then extrapolating the results at each stage to obtain the strain corresponding to zero diameter/height ratio.§ Since the barreling would theoretically disappear for a specimen of infinite height, the extrapolation method eliminates the frictional effect.

Homogeneous deformation in the simple compression test can be achieved by inserting PTFE (polytetra fluoroethylene) films of suitable thickness between the specimen and the compression platens. As well as producing effective lubrication, the PTFE films are themselves compressed so as to exert radial pressure to the material near the periphery. This inhibits the barreling tendency, except when the film thickness is too small. An excessive film thickness, on the other hand, produces bollarding in which the diameter of the specimen becomes bigger at the ends than at the middle. For a given specimen, there is an optimum film thickness for which neither barreling nor bollarding would occur. The compression should be carried out incrementally, renewing the PTFE films after each load application. Using the constancy of volume, the load required during the homogeneous compression may be written as

$$P = \sigma A = \frac{\sigma A_0 h_0}{h} = \frac{\sigma A_0}{1 - e}$$

where A_0 is the original area of cross section of the specimen. The graph for P against e shows an upward inflection and rises continuously without limit (Fig. 1.2*b*). Setting $d^2P/de^2 = 0$, and using the fact that $d/d\varepsilon = (1 - e)d/de$, the condition for inflection is found as

$$\left(\frac{d}{d\varepsilon} + 2\right)\left(\frac{d\sigma}{d\varepsilon} + \sigma\right) = 0 \tag{4}$$

† P. W. Bridgman, *Trans. A.S.M.E.*, **32**: 553 (1944); N. N. Davidenkov and N. I. Spiridonova, *Proc. Am. Soc. Test. Mat.*, **46**: 1147 (1946). See also E. R. Marshall and M. C. Shaw, *Trans. A.S.M.E.*, **44**: 716 (1952); J. D. Lubahn and R. P. Felgar, *Plasticity and Creep of Metals*, p. 114, Wiley and Sons, New York (1961).

‡ A dynamic analysis for the development of the neck has been given by N. K. Gupta and B. Karunes, *Int. J. Mech. Sci.*, **21**: 387 (1979).

§ The extrapolation method has been developed by G. Sachs, *Zeit. Metallkunde*, **16**: 55 (1924), M. Cook and E. C. Larke, *J. Inst. Metals*, **71**: 371 (1945), A. B. Watts and H. Ford, *Proc. Inst. Mech. Eng.*, **169**: 1141 (1955).

which defines the corresponding point on the true stress–strain curve. This point is most conveniently located if the stress–strain curve is represented by an empirical equation. In view of the incompressibility of the material, the nominal stress is $s = \sigma \exp(\varepsilon)$ in compression and $s = \sigma \exp(-\varepsilon)$ in tension.

The work done in changing the height of a specimen from h to $h + dh$ in simple compression is $-P\,dh$, where P is the current axial load. The incremental work done per unit volume of the specimen is therefore equal to $-P\,dh/Ah$ or $\sigma\,d\varepsilon$. It follows that during the homogeneous compression of a specimen from an initial height h_0 to a current height h, the work done per unit volume is given by the area under the true stress–strain curve up to a total strain of $\ln(h_0/h)$.

(iii) ***Empirical stress–strain equations*** For theoretical computations, it is often necessary to represent an experimentally determined stress–strain curve by an empirical equation of suitable form. When the material is rigid/plastic, it is frequently convenient to employ the Ludwik power law†

$$\sigma = C\varepsilon^n \tag{5}$$

where C is a constant stress, and n is a strain-hardening exponent usually lying between zero and 0.5. The equation predicts a zero initial stress and an infinite initial slope, except for $n = 0$ which represents a nonhardening rigid/plastic material. The higher the value of n, the more pronounced is the strain-hardening characteristic of the material (Fig. 1.3a). Since $d\sigma/d\varepsilon = n\sigma/\varepsilon$ in view of (5), it follows from (3) that the magnitude of the true strain at the onset of necking in simple tension is equal to n. The work done per unit volume during a homogeneous extension or contraction is easily shown to be $\sigma\varepsilon/(1 + n)$, where σ and ε are the final values of stress and strain.

The simple power law (5) may be readily modified by including a constant term Y representing the initial yield stress. The stress–strain equation then becomes

$$\sigma = Y(1 + m\varepsilon^n) \tag{6}$$

where m and n are dimensionless constants. Although this formula represents the strict rigid/plastic behavior of metals, it does not give a better fit for an actual stress–strain curve over a wide range of strains. When $n = 1$, the above equation represents a linear strain-hardening, which is a reasonable approximation for heavily prestrained metals. A more successful formula, due to Swift,‡ is the generalized power law

$$\sigma = C(m + \varepsilon)^n \tag{7}$$

where C, m, and n are empirical constants. The stress–strain curve represented by (7) can be obtained from that given by (5) if the stress axis is move along the positive strain axis through a distance m. Hence m may be regarded as the amount of prestrain

† P. Ludwik, *Elem. Technol. Mech.*, Springer Verlag, Berlin (1909).
‡ H. W. Swift, *J. Mech. Phys. Solids*, **1**: 1 (1952).

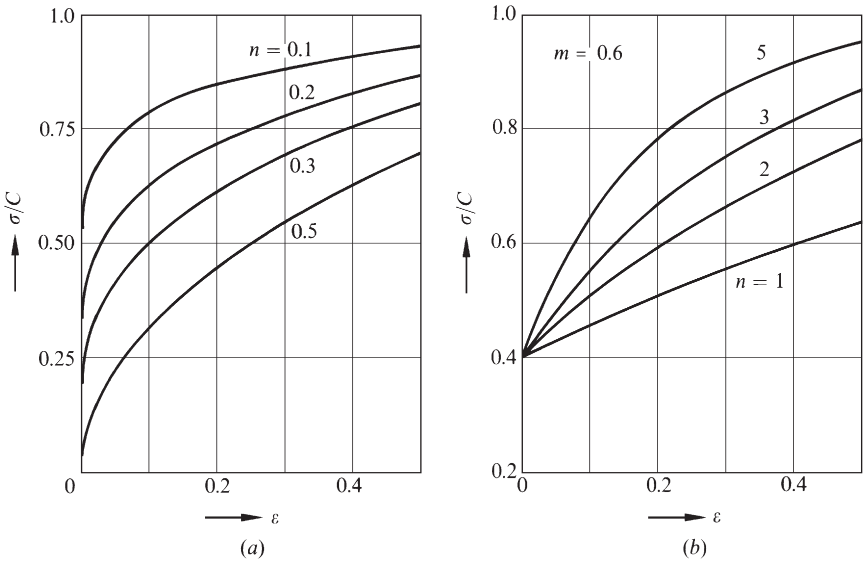

Figure 1.3 Empirical stress–strain curves for rigid/plastic materials. (*a*) Ludwik equation; (*b*) Voce equation.

in a material whose stress–strain curve in the annealed state corresponds to $m = 0$, the value of n remaining the same. If a given prestrained metal is represented by both (5) and (7), the value of n in the two cases will of course be different. The instability strain in simple tension according to the Swift equation is $n - m$ for $m \leqslant n$ and zero for $m \geqslant n$.

For certain applications involving rigid/plastic materials, it is convenient to use an equation suggested by Voce.† In its simplest form, the Voce equation may be written as

$$\sigma = C(1 - me^{-n\varepsilon}) \tag{8}$$

where e is the exponential constant. The curves corresponding to varying m and n approach the asymptote $\sigma = C$ (Fig. 1.3*b*). However, C is unlikely to be the saturation stress of a given metal as the rate of hardening becomes vanishingly small. The rapidity with which the asymptotic value is approached is represented by n. The coefficient m defines the initial state of hardening, the fully hardened material corresponding to $m = 0$. The slope of the stress–strain curve given by (8) is equal to $n(C - \sigma)$, which varies linearly with the stress.

When the elastic and plastic strains are of comparable magnitudes, it is necessary to replace ε in the preceding equations by the plastic strain ε^p. Considering the power law (5), the plastic part of the strain may be assumed to vary as σ^m, where $m = 1/n$, Since the elastic part of the strain is equal to σ/E, the total strain may be expressed

† E. Voce, *J. Inst. Metals*, **74**: 537 (1948). See also J. H. Palm, *Appl. Sci. Res.*, **A-2**: 198 (1948).

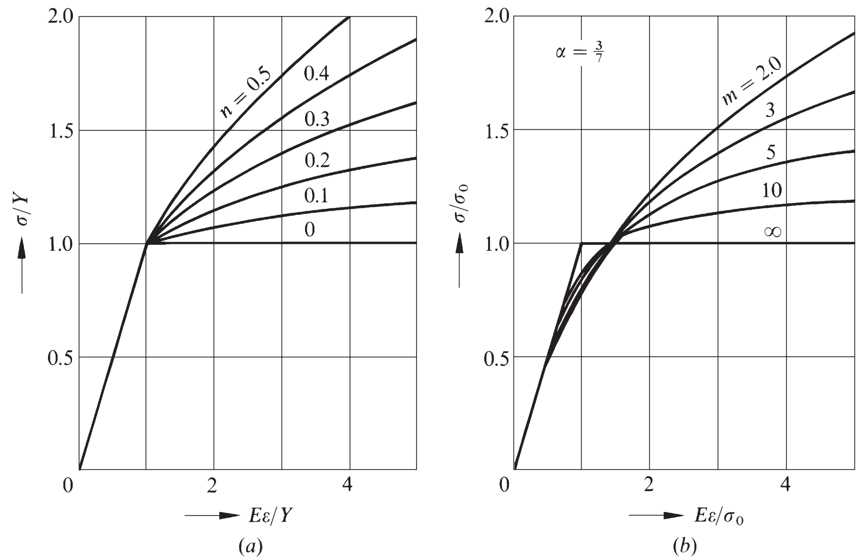

Figure 1.4 Empirical stress–strain curves for elastic/plastic materials. (*a*) Modified Ludwik equation; (*b*) Ramberg-Osgood equation.

by the Ramberg-Osgood equation†

$$\varepsilon = \frac{\sigma}{E}\left\{1 + \alpha\left(\frac{\sigma}{\sigma_0}\right)^{m-1}\right\} \tag{9}$$

where σ_0 is a nominal yield stress and α a dimensionless constant. The slope of the stress–strain curve given by the above equation continuously decreases from the value E at the origin (Fig. 1.4*b*). At the nominal yield point $\sigma = \sigma_0$, the plastic strain is α times the elastic strain, and the secant modulus is $E/(1+\alpha)$. The tangent modulus at any point of the curve is given by

$$\frac{E}{T} = 1 + \alpha m\left(\frac{\sigma}{\sigma_0}\right)^{m-1} \tag{10}$$

The second term on the right-hand side is equal to E/H in view of (1). The stress–strain curve for a range of materials can be reasonably fitted by Equation (9) with $\alpha = 3/7$. For a nonhardening material ($m = \infty$), the equation degenerates into a pair of straight lines meeting at the yield point $\sigma = \sigma_0$.

The contraction ratio η determined from (2) and (10) is plotted against $E\varepsilon/\sigma_0$ in Fig. 1.5, assuming $\alpha = 3/7$. Due to the nature of the Ramberg-Osgood equation, a variation of η is predicted even in the elastic range of straining. The contraction

† W. Ramberg and W. R. Osgood, *NACA Tech. Note*, 902 (1943).

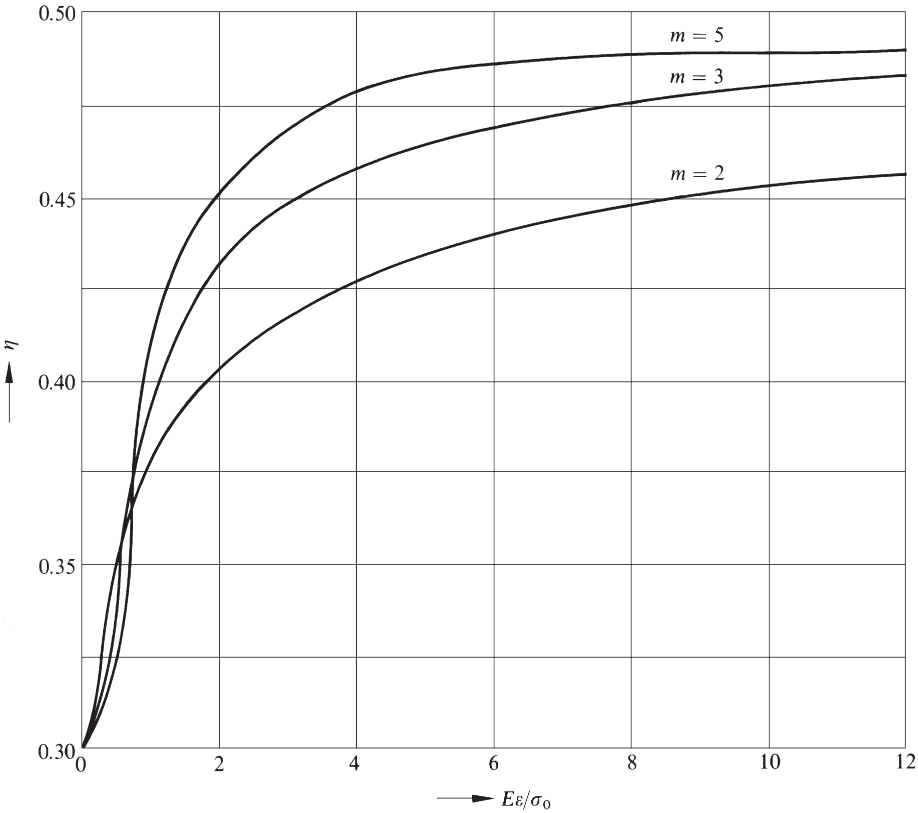

Figure 1.5 Variation of the contraction ratio with longitudinal strain in uniaxial tension according to the Ramberg-Osgood stress–strain equation ($\nu = 0.3$).

ratio increases very rapidly in the neighborhood of the yield point, following which η approaches the value 0.5 in an asymptotic manner. The actual value of η is seen to be reasonably close to 0.5 while the total strain is still of the elastic order of magnitude.

It is sometimes more convenient to employ a stress–strain equation where the curve in the plastic range is expressed by a simple power law, the material being assumed to have a definite yield point at $\sigma = Y$. The empirical representation then becomes

$$\sigma = \begin{cases} E\varepsilon & \varepsilon \leqslant \dfrac{Y}{E} \\ Y\left(\dfrac{E\varepsilon}{Y}\right)^n & \varepsilon \geqslant \dfrac{Y}{E} \end{cases} \tag{11}$$

where n is generally less than 0.5. The slope of the stress–strain curve given by (11) changes discontinuously from E to nE at the yield point (Fig. 1.4*a*). The tangent modulus at any point in the plastic range is n times the secant modulus. The empirical curve is effectively the Ludwik curve whose initial part is replaced by a chord of slope E.

The Ramberg-Osgood curve represents a continuous transition from the elastic to the plastic behavior expressed by a single equation when the material work-hardens. A similar curve for the ideally plastic material is given by the equation

$$\sigma = Y \tanh\left(\frac{E\varepsilon}{Y}\right)$$

which is due to Prager.† The curve having an initial slope E gradually bends over to approach the yield stress Y in an asymptotic manner. The approach is so rapid that σ is within 1 percent of Y when ε is only $4Y/E$. The tangent modulus at any point on the curve is equal to $E(1 - \sigma^2/Y^2)$, and the corresponding plastic modulus is $E(Y^2/\sigma^2 - 1)$. These moduli soon become negligible while the strain is still quite small.‡

(iv) ***Influence of pressure, strain rate, and temperature*** The tensile test of ductile materials under superimposed hydrostatic pressure has revealed that the yield point and the uniform elongation are unaffected by the applied pressure, but the strain to fracture increases with the intensity of the pressure. The increased ductility of the material is caused by the lateral compressive stresses which inhibit the formation of microcracks that lead to fracture. Test results for both tension and compression of brittle materials under fluid pressure indicate that there is a certain critical pressure above which the material behaves in a ductile manner.§ The stress–strain curves for axially compressed limestone cylinders under uniform fluid pressures acting on the curved surface are shown in Fig. 1.6, where σ denotes the axial compressive stress in excess of the confining pressure p. Each curve corresponds to a particular confining pressure expressed in atmospheres.¶ Some materials are found to suffer a certain amount of permanent volume change when subjected to hydrostatic pressures of exceedingly high magnitude, although the change is negligible in ordinary situations.‖

† W. Prager, *Rev. Fac. Sci.*, *Univ. Istanbul*, **5**: 215 (1941); *Duke Math. J.*, **9**: 228 (1942).

‡ Other forms of stress–strain equation are sometimes used for the derivation of special solutions. See, for example, R. Hill, *Phil. Mag.*, **41**: 1133 (1950), and J. Chakrabarty, *Int. J. Mech. Sci.*, **12**: 315 (1970).

§ The pressure can be accurately measured from the change in resistance of a manganin wire immersed in the pressurized fluid. A detailed account of the experimental investigations regarding the effect of hydrostatic pressure on metals has been presented by P. W. Bridgman, *Studies in Large Plastic Flow and Fracture*, McGraw-Hill Book Company, New York (1952), and by H. Ll. D. Pugh (ed.), *Mechanical Behavior of Materials under Pressure*, Elsevier, Amsterdam (1970).

¶ Experimental results on the compression of marble and limestone cylinders under fluid pressure have been reported by Th. von Karman, *Z. Ver. deut. Ing.*, **55**: 1749 (1911), and by D. T. Griggs, *J. Geol.*, **44**: 541 (1936).

‖ P. W. Bridgman, *J. Appl. Phys.*, **18**: 246 (1947). The effect of hydrolastic pressure on the shear properties of metals has been investigated by B. Crossland, *Proc. Inst. Mech. Eng.*, **169**: 935 (1954); B. Crossland and W. H. Dearden, ibid., **172**, 805 (1958). See also M. C. Shaw, *Int. J. Mech. Sci.*, **22**: 673 (1980).

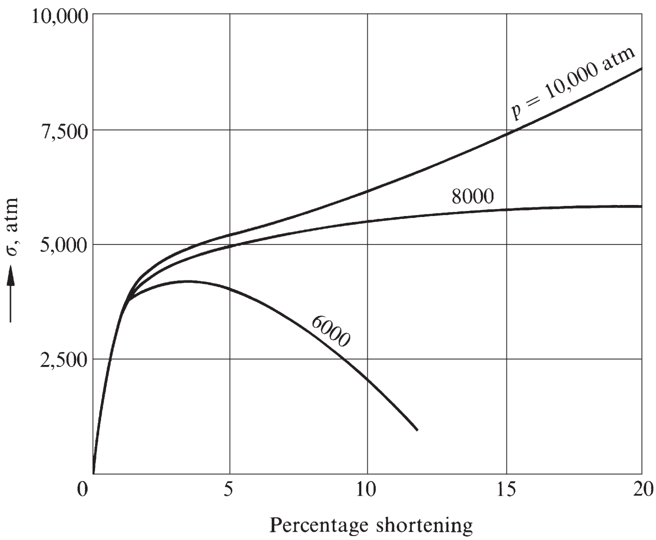

Figure 1.6 Behavior of limestone cylinders under axial thrust and lateral pressure (*after Griggs*).

Plastic instability is found to occur in cylindrical bars when subjected to lateral fluid pressures of sufficient magnitude.† The phenomenon is caused by a slight non-uniformity in distortion of the unconstrained surface which is exposed to fluid pressure. When the material is ductile, the longitudinal strain at the onset of necking is exactly the same as that in uniaxial tension, but the cross section of the neck is greatly reduced before fracture. Brittle materials, which normally fracture with no significant plastic strain under simple tension, are found to deform beyond the point of necking when tested under lateral fluid pressure. Moreover, the uniform strain at the onset of necking is found to be identical to that given by (3), with the stress–strain curve obtained in simple compression. For extremely brittle materials, the fracture mode seems to remain brittle even under a fluid pressure acting on the lateral surface.‡

At room temperature, the stress–strain curve of metals is practically independent of the rate of straining attainable in ordinary testing machines. High-speed tensile tests have shown that the yield stress increases with the strain rate, and this effect is more pronounced at elevated temperatures. The true strain rate in simple compression is defined as $\dot{\varepsilon} = -\dot{h}/h$, where h is the current specimen height and $\dot{h}$ its rate of change. To obtain a constant strain rate during a test, it is therefore necessary to decrease the platen speed in proportion to the specimen height. This is achieved by using a cam plastometer in which one of the compression platens is actuated by a cam of logarithmic profile.§ Maintaining a constant temperature during a test is

† J. Chakrabarty. *Proc. 13th Int. M.T.D.R. Conf.*, p. 565, Pergamon Press, Oxford (1972).

‡ P. W. Bridgman, *Phil. Mag.*, July, 63 (1912).

§ The cam plastometer has been devised by E. Orowan, Brit. Iron and Steel Res. Assoc. Rep., MW/F/22 (1950).

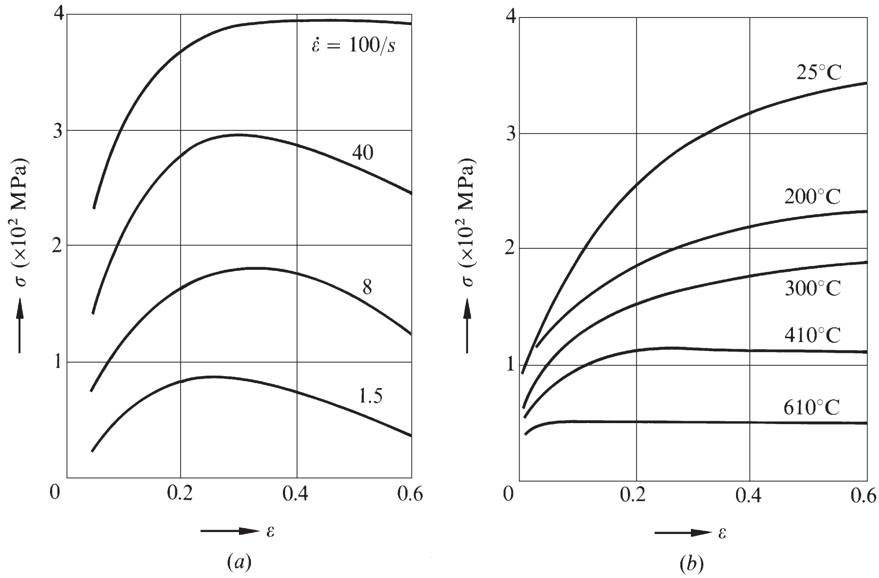

Figure 1.7 Effects of strain rate and temperature on the stress–strain curve of metals. (*a*) EN25 steel at 1000°C (*after Cook*); (*b*) annealed copper at a strain rate of $10^{-3}/s$ (*after Mahtab et al.*).

more difficult, since the heat generated during the test raises the temperature of the specimen adiabatically. Figure 1.7 shows typical stress–strain curves of metals in compression, obtained under constant temperatures and strain rates.†

For a given value of the strain, the combined effect of strain rate and temperature on the yield stress may be expressed by the functional relationship‡

$$\sigma = f\left\{\dot{\varepsilon}\exp\left(\frac{Q}{RT}\right)\right\} \tag{12}$$

where Q is an activation energy for plastic flow, T the absolute testing temperature, and R the universal gas constant equal to 8.314 J/g mol °K. The above relationship has been experimentally confirmed for several metals over wide ranges of strain rate

† For experimental methods and results on the high-speed compression at elevated temperatures, see P. M. Cook, *Proc. Conf. Properties of Materials at High Rates of Strain*, *Inst. Mech. Eng.*, 86 (1957); F. U. Mahtab, W. Johnson, and R. A. C. Slater, *Proc. Inst. Mech. Eng.*, **180**: 285 (1965); S. K. Samanta, *Int. J. Mech. Sci.*, **10**: 613 (1968), *J. Mech. Phys. Solids*, **19**: 117 (1971); T. A. Dean and C. E. N. Sturgess, *Proc. Inst. Mech. Eng.*, **187**: 523 (1973). See also R. A. C. Slater, *Engineering Plasticity*, Chap. 6, Wiley and Sons, London (1977); M. S. J. Hashmi, *J. Strain Anal.*, **15**: 201 (1980).

‡ C. Zener and J. H. Hollomon, *J. Appl. Phys.*, **15**: 22 (1944); T. Trozera, O. D. Sherby, and J. L. Dorn, *Trans. ASME*, **49**: 173 (1957). The expression in the curly bracket of (12) is often called the Zener-Hollomon parameter, which is also useful in the theory of high-temperature creep. A generalized constitutive equation, including the effect of strain, has been discussed by J. M. Alexander, *Plasticity Today* (Ed. H. Sawczick), Elsevier, Amsterdam (1986).

and temperature. When the temperature is held constant, the test results can be fitted by the power law†

$$\sigma = C\varepsilon^n \dot{\varepsilon}^m \tag{13}$$

where C, m and n depend on the operating temperature. The exponent m is known as the *strain-rate sensitivity*, which generally increases with temperature, particularly when it is above the recrystallization temperature. The strain-hardening exponent n, on the other hand, rapidly decreases with increasing values of the elevated temperature.

The dependence of the flow stress on strain rate and temperature for a given strain is sometimes expressed in the alternative form‡

$$\sigma = f\left\{T\left(1 - m\ln\frac{\dot{\varepsilon}}{\dot{\varepsilon}_0}\right)\right\} \tag{14}$$

where m and $\dot{\varepsilon}_0$ are constants, the quantity in the curly bracket being known as the velocity modified temperature. It is consistent with the fact that an increase in strain rate is in effect equivalent to a decrease in temperature. Equation (14) agrees with test data for a fairly wide range of values of the strain rate and temperature.

Above the recrystallization temperature, the yield stress attains a saturation value after a small amount of strain, as a result of the work-hardening rate being balanced by the rate of thermal softening. The dependence of the saturation stress on strain rate and temperature can be expressed with reasonable accuracy by the empirical equation§

$$\sigma = C\sinh^{-1}\left(m\dot{\varepsilon}^n \exp\frac{b}{T}\right)$$

where b, C, m, and n are material constants. The activation energy Q is then independent of the temperature, and is approximately equal to Rb/n. A distinction between cold- and hot-working of metals is usually made on the basis of the recrystallization temperature, whose absolute value is roughly one-half of the absolute melting temperature. The above equation reduces to a power law when the expression in the parenthesis is sufficiently small.¶

† W. F. Hosford and R. M. Caddell, *Metal Forming Mechanics and Metallurgy*, 2d ed., Chap. 5, Prentice-Hall, Englewood Cliffs, NJ (1993).

‡ C. W. MacGregor and J. C. Fisher, *J. Appl. Mech.*, **13**: 11 (1946).

§ C. M. Sellars and W. J. McG. Tegart, *Mem. Sci. Rev. Met.*, **63**: 731 (1966); S. K. Samanta, *Proc. 11th Int. M.T.D.R. Conf.*, Pergamon Press, Oxford (1970).

¶ Large neck-free extensions are possible in certain highly rate-sensitive alloys, called *superplastic alloys.* See W. A. Backofen, I. Turner and H. Avery, *Trans. Q. ASM*, **57**: 981 (1966); J. W. Edington, K. N. Melton, and C. P. Cutler, *Prog. Mater. Sci.*, **21**: 63 (1976); K. A. Padmanabhan and G. J. Davies, *Superplasticity*, Springer-Verlag, Berlin (1980); T. G. Nieh, J. Wadsworth, and O. D. Sherby, *Superplasticity in Metals and Ceramics*, Cambridge University Press, Cambridge (1997).

1.3 Analysis of Stress

(i) ***Stress tensor*** When a body is subjected to a set of external forces, internal forces are produced in different parts of the body so that each element of the body is in a state of statical equilibrium. Through any point O within the body, consider a small surface element δS whose orientation is specified by the unit vector $\mathbf{l}$ along the normal drawn on one side of the element (Fig. 1.8*a*). The material on this side of δS may be regarded as exerting a force $\delta\mathbf{P}$ across the surface element upon the material on the other side. The limit of the ratio $\delta\mathbf{P}/\delta S$ as δS tends to zero is the stress vector $\mathbf{T}$ at O associated with the direction $\mathbf{l}$. For given external loading, the stress acting across any plane passing through a given point O depends on the orientation of the plane. The resolved component of the stress vector along the unit normal $\mathbf{l}$ is called the direct or normal stress denoted by σ, while the component tangential to the plane is known as the shear stress denoted by τ.

Consider now a set of rectangular axes Ox, Oy, and Oz emanating from a typical point O, and imagines a small rectangular parallelepiped at O having its edges parallel to the axes of reference (Fig. 1.8*b*). The normal stresses across the faces of the block are denoted by σ_x, σ_y, and σ_z, where the subscripts denote the directions of the normal to the faces. The shear stress acting on the faces normal to the x axis is resolved into the components τ_{xy} and τ_{xz} parallel to the y and z axes respectively. The first suffix denotes the direction of the normal to the face and the second suffix the direction of the component. In a similar way, the shear stresses on the faces normal to the y axis are denoted by τ_{yx} and τ_{yz}, and those on the faces normal to the z axis by τ_{zx} and τ_{zy}. The stresses are taken as positive if they are directed as shown in the figure, when the outward normals to the faces are in the positive directions of the coordinate axes. The positive directions are all reversed on the remaining faces of the block where the outward normals are in the negative directions of the axes of reference. The nine components of the stress at any point form a second-order tensor σ_{ij}, known as the stress tensor, where i and j take integral

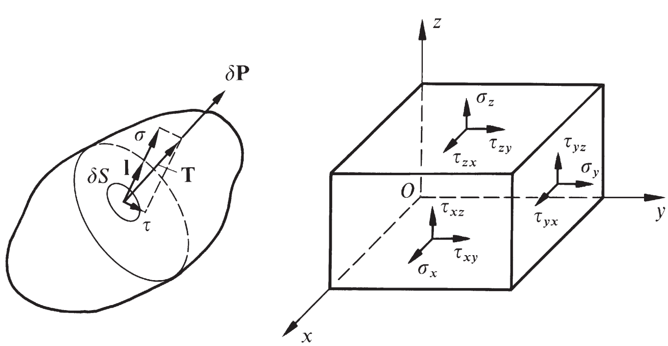

(*a*) (*b*)

Figure 1.8 Definition of stress. (*a*) Normal and shear stresses; (*b*) components of stress tensor.

values 1, 2, and 3. The stress components may be displayed as elements of the square matrix

$$\sigma_{ij} = \begin{bmatrix} \sigma_x & \tau_{xy} & \tau_{xz} \\ \tau_{yx} & \sigma_y & \tau_{yz} \\ \tau_{zx} & \tau_{zy} & \sigma_z \end{bmatrix} = \begin{bmatrix} \sigma_{11} & \sigma_{12} & \sigma_{13} \\ \sigma_{21} & \sigma_{22} & \sigma_{23} \\ \sigma_{31} & \sigma_{32} & \sigma_{33} \end{bmatrix}$$

The forces acting on the faces of the parallelepiped are clearly in equilibrium. To examine the couple equilibrium, let $\delta x, \delta y, \delta z$ denote the lengths of these faces along the respective coordinate axes. Then the resultant couple about the z axis is $(\tau_{xy} - \tau_{yx})\delta x\ \delta y\ \delta z$, which must vanish for equilibrium. This gives $\tau_{xy} = \tau_{yx}$. Similarly, the conditions for couple equilibrium about the other two axes give $\tau_{yz} = \tau_{zy}$ and $\tau_{zx} = \tau_{xz}$. These identities may be expressed as $\sigma_{ij} = \sigma_{ji}$, implying that the stress tensor is symmetric with respect to its subscripts. Thus there are six independent stress components, three normal components σ_x, σ_y, σ_z, and three shear components τ_{xy}, τ_{yz}, τ_{zx}, which completely specify the state of stress at each point of the body. The matrix representing the stress tensor is evidently symmetrical.

The mean of the three normal stresses, equal to $(\sigma_x + \sigma_y + \sigma_z)/3$, is known as the *hydrostatic stress* denoted by σ_0. A *deviatoric* or *reduced stress* tensor s_{ij} is defined as that which is obtained from σ_{ij} by reducing the normal stress components by σ_0. This gives the deviatoric stresses as

$$s_{ij} = \begin{bmatrix} s_x & s_{xy} & s_{xz} \\ s_{yx} & s_y & s_{yz} \\ s_{zx} & s_{zy} & s_z \end{bmatrix} = \begin{bmatrix} (\sigma_x - \sigma_0) & \tau_{xy} & \tau_{xz} \\ \tau_{yx} & (\sigma_y - \sigma_0) & \tau_{yz} \\ \tau_{zx} & \tau_{zy} & (\sigma_z - \sigma_0) \end{bmatrix}$$

The deviatoric normal stresses are therefore given by

$$3s_x = 2\sigma_x - \sigma_y - \sigma_z, \qquad 3s_y = 2\sigma_y - \sigma_z - \sigma_x, \qquad 3s_z = 2\sigma_z - \sigma_x - \sigma_y$$

The deviatoric shear stresses are the same as the actual shear stresses. Since $s_x + s_y + s_z = 0$, the deviatoric normal stresses cannot all have the same sign. The difference between any two normal components of the deviatoric stress is the same as that between the corresponding components of the actual stress. Expressed in suffix notation, the relationship between s_{ij} and σ_{ij} is

$$s_{ij} = \sigma_{ij} - \sigma_0\delta_{ij} = \sigma_{ij} - \tfrac{1}{3}\sigma_{kk}\delta_{ij} \tag{15}$$

where δ_{ij} is the *Kronecker delta* whose value is unity when $i = j$ and zero when $i \neq j$. Evidently, $\delta_{ij} = \delta_{ji}$. Any repeated or dummy suffix indicates a summation of all terms obtainable by assigning the values 1, 2, and 3 to this suffix in succession. Thus $\sigma_{kk} = \sigma_x + \sigma_y + \sigma_z$. It follows from the definition of the delta symbol that $\sigma_{ij}\delta_{jk} = \sigma_{ik}$, where j is a dummy suffix and i, k are free suffixes. Each term of a tensor equation must have the same free suffixes, but a dummy suffix can be replaced by any other letter different from the free suffixes.

(ii) ***Stresses on an oblique plane*** Consider the equilibrium of a small tetrahedron $OABC$ of which the edges OA, OB, and OC are along the coordinate axes (Fig. 1.9). Let (l, m, n) be the directions cosines of a straight line drawn along the exterior normal to the oblique plane ABC. These are the components of the unit normal **1** with respect to Ox, Oy, and Oz. If the area of the face ABC is denoted by δS, the faces OAB, OBC, and OCA have areas $n\,\delta S, l\,\delta S$, and $m\,\delta S$ respectively. The stress vector **T** acting across the face ABC has components T_x, T_y, and T_z along the axes of reference. Resolving the forces in the directions Ox, Oy, and Oz, we get

$$\begin{aligned} T_x &= l\sigma_x + m\tau_{xy} + n\tau_{zx} \\ T_y &= l\tau_{xy} + m\sigma_y + n\tau_{yz} \\ T_z &= l\tau_{zx} + m\tau_{yz} + n\sigma_z \end{aligned} \tag{16}$$

on cancelling out δS from each equation of force equilibrium. When δS tends to zero, these equations give the components of the stress vector at O, associated with the direction (l, m, n), in terms of the components of the stress tensor. Using the suffix notation and the summation convention, (16) can be expressed as

$$T_j = l_i \sigma_{ij}$$

where $l_1 = l$, $l_2 = m$, $l_3 = n$. The above equation is equivalent to three equations corresponding to the three possible values of the free suffix j. A single free suffix therefore characterizes a vector. The normal stress across the plane specified by its

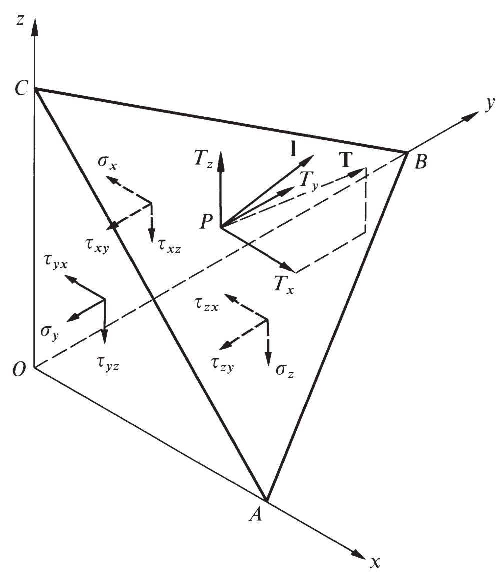

Figure 1.9 Stresses across an oblique plane in a three-dimensional state of stress.

normal (l, m, n) is

$$\begin{aligned}\sigma &= lT_x + mT_y + nT_z = l_j T_j = l_i l_j \sigma_{ij} \\ &= l^2\sigma_x + m^2\sigma_y + n^2\sigma_z + 2lm\tau_{xy} + 2mn\tau_{yz} + 2nl\tau_{zx}\end{aligned} \tag{17}$$

The shear stress across the plane can be resolved into two components in a pair of mutually perpendicular directions in the plane. Denoting one of these directions by (l', m', n'), the corresponding shear component is obtained as

$$\begin{aligned}\tau' &= l'T_x + m'T_y + n'T_z = l'_j T_j = l_i l'_j \sigma_{ij} \\ &= ll'\sigma_x + mm'\sigma_y + nn'\sigma_z + (lm' + ml')\tau_{xy} + (mn' + nm')\tau_{yz} + (nl' + ln')\tau_{zx}\end{aligned} \tag{18}$$

This evidently is the resolved component of the resultant stress in the direction (l', m', n'). The direction cosines satisfy the well-known geometrical relations

$$l^2 + m^2 + n^2 = 1 \qquad l'^2 + m'^2 + n'^2 = 1 \qquad ll' + mm' + nn' = 0 \tag{19}$$

The first two equations express the fact (l, m, n) and (l', m', n') represent unit vectors, while the last relation expresses the orthogonality of these vectors. The shear stress is most conveniently found from the fact that its magnitude is $\sqrt{T^2 - \sigma^2}$, and its direction cosines are proportional to its rectangular components

$$T_x - l\sigma \qquad T_y - m\sigma \qquad T_z - n\sigma$$

Let x_i and x'_i represent two sets of rectangular axes through a common origin O, and a_{ij} denote the direction cosine of the x'_i axis with respect to the x_j axis. The direction cosine of the x_i axis with respect to the x'_j axis is then equal to a_{ji}. It follows from geometry that the coordinates of any point in space referred to the two sets of axes are related by the equations

$$x'_i = a_{ij}x_j \qquad x_j = a_{ij}x'_i \tag{20}$$

The components of any vector transform† according to the same law as (20). Let σ'_{ij} denote the components of the stress tensor when referred to the set of axes x'_i. A defining property of tensors is the transformation law

$$\sigma'_{ij} = a_{ik}a_{jl}\sigma_{kl} \tag{21}$$

Let us suppose that $a_{11} = l$, $a_{12} = m$, $a_{13} = n$, and $a_{21} = l'$, $a_{22} = m'$, $a_{23} = n'$. The normal stress across the plane (l, m, n) is then equal to σ'_{11}, and the corresponding expression (17) can be readily verified from (21). Similarly, the component of the shear stress across the plane resolved in the direction (l', m', n') is equal to σ'_{12} which can be shown to be that given by (18).

† It follows from (20) that $x'_i = a_{ik}x_k = a_{ik}a_{jk}x'_j$, indicating that $a_{ik}a_{jk} = \delta_{ij}$, which furnishes six independent relations of types (19).

(iii) ***Principal stresses*** The normal stress σ has maximum and minimum values for varying orientations of the oblique plane. Regarding l and m as the independent direction cosines, the conditions for stationary σ may be written as $\partial\sigma/\partial l = 0$, $\partial\sigma/\partial m = 0$. Differentiating the first equation of (19) partially with respect to l and m, we get $\partial n/\partial l = -l/n$ and $\partial n/\partial m = -m/n$. Inserting these results into the partial derivatives of (17), and using (16), the stationary condition can be expressed as

$$\frac{T_x}{l} = \frac{T_y}{m} = \frac{T_z}{n}$$

This shows that the resultant stress across the plane acts in the direction of the normal when the normal stress has a stationary value. Each of the above ratios is therefore equal to the normal stress σ. The substitution into (16) gives

$$\begin{aligned} l(\sigma_x - \sigma) + m\tau_{xy} + n\tau_{zx} &= 0 \\ l\tau_{xy} + m(\sigma_y - \sigma) + n\tau_{yz} &= 0 \\ l\tau_{zx} + m\tau_{yz} + n(\sigma_z - \sigma) &= 0 \end{aligned} \tag{22}$$

In suffix notation, these relations are equivalent to $l_i(\sigma_{ij} - \sigma\delta_{ij}) = 0$, which follows directly from the fact that $T_j = \sigma l_j$ across a principal plane. The set of linear homogeneous equations (22) would have a nonzero solution for l, m, n if the determinant of their coefficients vanishes. Thus

$$\begin{vmatrix} \sigma_x - \sigma & \tau_{xy} & \tau_{zx} \\ \tau_{xy} & \sigma_y - \sigma & \tau_{yz} \\ \tau_{zx} & \tau_{yz} & \sigma_z - \sigma \end{vmatrix} = 0$$

Expanding this determinant, we obtain a cubic equation in σ having three real roots σ_1, σ_2, σ_3, which are known as the *principal stresses*. These stresses act across planes on which the shear stresses are zero. The cubic may be expressed in the form

$$\sigma^3 - I_1\sigma^2 - I_2\sigma - I_3 = 0 \tag{23}$$

where

$$I_1 = \sigma_x + \sigma_y + \sigma_z = \sigma_1 + \sigma_2 + \sigma_3 = \sigma_{ii} \tag{24}$$

$$\begin{aligned} I_2 &= -(\sigma_x\sigma_y + \sigma_y\sigma_z + \sigma_z\sigma_x) + \tau_{xy}^2 + \tau_{yz}^2 + \tau_{zx}^2 \\ &= -(\sigma_1\sigma_2 + \sigma_2\sigma_3 + \sigma_3\sigma_1) = \tfrac{1}{2}(\sigma_{ij}\sigma_{ij} - \sigma_{ii}\sigma_{jj}) \end{aligned} \tag{25}$$

$$\begin{aligned} I_3 &= \sigma_x\sigma_y\sigma_z + 2\tau_{xy}\tau_{yz}\tau_{zx} - \sigma_x\tau_{yz}^2 - \sigma_y\tau_{zx}^2 - \sigma_z\tau_{xy}^2 \\ &= \begin{vmatrix} \sigma_x & \tau_{xy} & \tau_{zx} \\ \tau_{xy} & \sigma_y & \tau_{yz} \\ \tau_{zx} & \tau_{yz} & \sigma_z \end{vmatrix} = \sigma_1\sigma_2\sigma_3 \end{aligned} \tag{26}$$

The expressions for I_1, I_2, I_3 in terms of the principal stresses follow from the fact that (23) is equivalent to the equation $(\sigma-\sigma_1)(\sigma-\sigma_2)(\sigma-\sigma_3)=0$. Since the stationary values of the normal stress do not depend on the orientation of the coordinate axes, the coefficients of (23) must also be independent of the choice of the axes of references. The quantities I_1, I_2, I_3 are therefore known as the *invariants* of the stress tensor.†

The direction cosines corresponding to each principal stress can be found from the first equation of (19) and any two equations of (22) with the appropriate value of σ. Let (l_1, m_1, n_1) and (l_2, m_2, n_2) represent the directions of σ_1 and σ_2 respectively. If we express (22) in terms of l_1, m_1, n_1, and σ_1, multiply these equations by l_2, m_2, n_2 in order and add them together, and then subtract the resulting equation from that obtained by interchanging the subscripts, we arrive at the result

$$(\sigma_1-\sigma_2)(l_1l_2+m_1m_2+n_1n_2)=0$$

If $\sigma_1 \neq \sigma_2$, the above equation indicates that the directions (l_1, m_1, n_1) and (l_2, m_2, n_2) are perpendicular to one another. It follows, therefore, that the principal directions corresponding to distinct values of the principal stresses are mutually orthogonal. These directions are known as the *principal axes* of the stress. When two of the principal stresses are equal to one another, the direction of the third principal stress is uniquely determined, but all directions perpendicular to this principal axis are principal directions. When $\sigma_1=\sigma_2=\sigma_3$, representing a hydrostatic state of stress, any direction in space is a principal direction.

The invariants of the deviatoric stress tensor are obtained by replacing the actual stress components in (24) to (26) by the corresponding deviatoric components. The first deviatoric stress invariant is

$$J_1 = s_x+s_y+s_z = s_1+s_2+s_3 = s_{ii} = 0$$

where s_1, s_2, s_3 are the principal deviatoric stresses. These principal values are the roots of the cubic equation

$$s^3 - J_2 s - J_3 = 0 \tag{27}$$

where

$$\begin{aligned} J_2 &= -(s_xs_y+s_ys_z+s_zs_x)+\tau_{xy}^2+\tau_{yz}^2+\tau_{zx}^2 \\ &= \tfrac{1}{2}(s_x^2+s_y^2+s_z^2)+\tau_{xy}^2+\tau_{yz}^2+\tau_{zx}^2 \\ &= \tfrac{1}{6}[(\sigma_x-\sigma_y)^2+(\sigma_y-\sigma_z)^2+(\sigma_z-\sigma_x)^2]+\tau_{xy}^2+\tau_{yz}^2+\tau_{zx}^2 \end{aligned} \tag{28}$$

$$\begin{aligned} J_3 &= s_xs_ys_z+2\tau_{xy}\tau_{yz}\tau_{zx}-s_x\tau_{yz}^2-s_y\tau_{zx}^2-s_z\tau_{xy}^2 \\ &= \begin{vmatrix} s_x & \tau_{xy} & \tau_{zx} \\ \tau_{xy} & s_y & \tau_{yz} \\ \tau_{zx} & \tau_{yz} & s_z \end{vmatrix} = s_1s_2s_3 = \tfrac{1}{3}(s_1^3+s_2^3+s_3^3) \end{aligned} \tag{29}$$

† Any symmetric tensor of second order has three real principal values, the basic invariants of the tensor being identical in form to those for the stress.

The last two expressions for J_2 are obtained from the first expression by adding the identically zero terms $\frac{1}{2}(s_x + s_y + s_z)^2$ and $\frac{1}{3}(s_x + s_y + s_z)^2$ respectively, and noting the fact that $s_x - s_y = \sigma_x - \sigma_y$ etc. Similarly, the last expression for J_3 follows from the preceding one on adding the term $\frac{1}{3}(s_1 + s_2 + s_3)^3$. In suffix notation, these invariants can be written as

$$J_2 = \tfrac{1}{2}s_{ij}s_{ij} \qquad J_3 = \tfrac{1}{3}s_{ij}s_{jk}s_{ki} \tag{30}$$

The repetition of all suffixes is a characteristic of invariants, which are scalars. Substituting $\sigma = s + I_1/3$ in (23) and comparing the coefficients of the resulting equation with those of (27), we obtain

$$J_2 = I_2 + \tfrac{1}{3}I_1^2 \qquad J_3 = I_3 + \tfrac{1}{3}I_1I_2 + \tfrac{2}{27}I_1^3$$

When J_2 and J_3 have been found, equation (27) may be solved by means of the substitution $s = 2\sqrt{J_2/3}\cos\phi$, which reduces the cubic to

$$\cos 3\phi = \frac{J_3}{2}\left(\frac{3}{J_2}\right)^{3/2} \tag{31}$$

Since $4J_2^3 \geqslant 27J_3^2$, the right-hand side† of (31) lies between -1 and 1, and one value of ϕ lies between 0 and $\pi/3$. The principal deviatoric stresses may therefore be written as

$$s_1 = 2\sqrt{\frac{J_2}{3}}\cos\phi \qquad s_2, s_3 = -2\sqrt{\frac{J_2}{3}}\cos\left(\frac{\pi}{3} \pm \phi\right) \tag{32}$$

where $0 \leqslant \phi \leqslant \pi/3$. Any function of these principal components is also a function of the invariants, which play an important part in the mathematical development of the theory of plasticity.

(iv) ***Principal shear stresses*** When the principal stresses and their directions are known, it is convenient to take the principal axes as the axes of reference. If Ox, Oy, Oz denote the coordinate axes associated with the principal stresses σ_1, σ_2, σ_3 respectively, the components of the stress vector across a plane whose normal is in the direction (l, m, n) are

$$T_x = l\sigma_1 \qquad T_y = m\sigma_2 \qquad T_z = n\sigma_3$$

The normal stress across the oblique plane therefore becomes

$$\sigma = l^2\sigma_1 + m^2\sigma_2 + n^2\sigma_3 \tag{33}$$

† Using (32) and (31), it can be shown that $4J_2^3 - 27J_3^2 = (\sigma_1 - \sigma_2)^2(\sigma_2 - \sigma_3)^2(\sigma_3 - \sigma_1)^2$, which is a positive quantity for distinct values of the principal stresses.

If the magnitude of the shear stress across the plane is denoted by τ, then

$$\tau^2 = T^2 - \sigma^2 = (l^2\sigma_1^2 + m^2\sigma_2^2 + n^2\sigma_3^2) - (l^2\sigma_1 + m^2\sigma_2 + n^2\sigma_3)^2$$
$$= (\sigma_1 - \sigma_2)^2 l^2 m^2 + (\sigma_2 - \sigma_3)^2 m^2 n^2 + (\sigma_3 - \sigma_1)^2 n^2 l^2 \tag{34}$$

in view of the relation $l^2 + m^2 + n^2 = 1$. Since the components of the normal stress along the coordinate axes are $(l\sigma, m\sigma, n\sigma)$, the components of the shear stress are $l(\sigma_1 - \sigma), m(\sigma_2 - \sigma), n(\sigma_3 - \sigma)$. Hence the direction cosines of the shear stress are

$$l_s = l\left(\frac{\sigma_1 - \sigma}{\tau}\right) \qquad m_s = m\left(\frac{\sigma_2 - \sigma}{\tau}\right) \qquad n_s = n\left(\frac{\sigma_3 - \sigma}{\tau}\right) \tag{35}$$

A plane which is equally inclined to the three principal axes is known as the *octahedral plane*, the direction cosines of its normal being given by $l^2 = m^2 = n^2 = 1/3$. These relations are satisfied by four pairs of parallel planes forming a regular octahedron having its vertices on the principal axes. By (33) and (34), the octahedral normal stress is equal to the hydrostatic stress σ_0, and the octahedral shear stress is of the magnitude

$$\tau_0 = \tfrac{1}{3}\sqrt{(\sigma_1 - \sigma_2)^2 + (\sigma_2 - \sigma_3)^2 + (\sigma_3 - \sigma_1)^2} = \sqrt{\tfrac{2}{3}J_2}$$

The components of the octahedral shear stress along the principal axes are numerically equal to $1/\sqrt{3}$ times the deviatoric principal stresses.

We now proceed to determine the stationary values of the shear stress for varying orientations of the oblique plane. To this end, we put $n^2 = 1 - l^2 - m^2$ in (34), and express it in the form

$$\tau^2 = l^2(\sigma_1^2 - \sigma_3^2) + m^2(\sigma_2^2 - \sigma_3^2) + \sigma_3^2 - \{l^2(\sigma_1 - \sigma_3) + m^2(\sigma_2 - \sigma_3) + \sigma_3\}^2$$

where l and m are treated as the independent variables. We shall follow the convention $\sigma_1 > \sigma_2 > \sigma_3$. Equating to zero the derivatives of τ^2 with respect to l and m, we obtain

$$\begin{aligned} l(\sigma_1 - \sigma_3)[(1 - 2l^2)(\sigma_1 - \sigma_3) - 2m^2(\sigma_2 - \sigma_3)] &= 0 \\ m(\sigma_2 - \sigma_3)[(1 - 2m^2)(\sigma_2 - \sigma_3) - 2l^2(\sigma_1 - \sigma_3)] &= 0 \end{aligned} \tag{36}$$

These equations are obviously satisfied for $l = m = 0$, and hence $n = 1$, which corresponds to a principal stress direction for which the shear stress has a minimum value of zero. To obtain a maximum value of the shear stress, we set $l = 0$ satisfying the first equation of (36), and use this value in the second equation to get $l - 2m^2 = 0$. This gives $l = 0, m^2 = n^2 = 1/2$ corresponding to maximum shear stress equal to $\frac{1}{2}(\sigma_2 - \sigma_3)$ according to (34). Similarly, the direction represented by $m = 0$, $n^2 = l^2 = 1/2$ satisfies (36), and furnishes a maximum value of $\frac{1}{2}(\sigma_1 - \sigma_3)$ for the shear stress. Finally, setting $n = 0$ and hence $l^2 + m^2 = 1$, we find that τ is a maximum for $l^2 = m^2 = 1/2$, giving a stationary value equal to $\frac{1}{2}(\sigma_1 - \sigma_2)$. The three

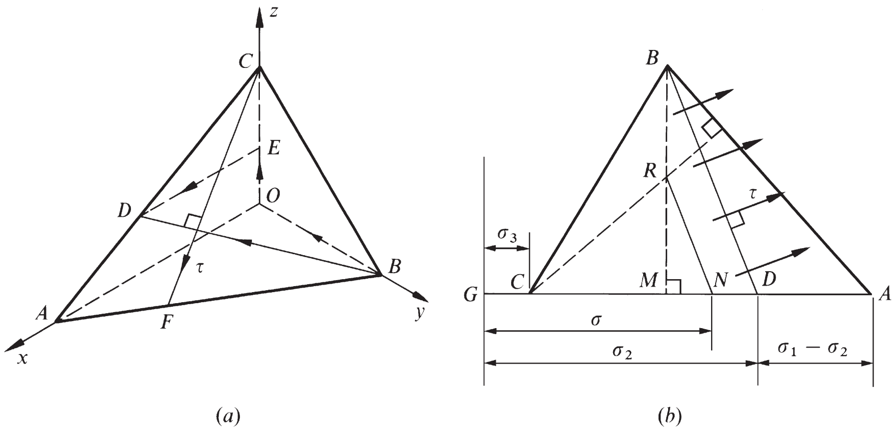

Figure 1.10 Construction for the normal stress and the direction of the shear stress.

stationary shear stresses, known as the *principal shear stresses*, may therefore be written as

$$\tau_1 = \tfrac{1}{2}(\sigma_2 - \sigma_3) \qquad \tau_2 = \tfrac{1}{2}(\sigma_1 - \sigma_3) \qquad \tau_3 = \tfrac{1}{2}(\sigma_1 - \sigma_2) \tag{37}$$

These stresses act in directions which bisect the angles between the principal axes. By (33), the normal stresses acting on the planes of τ_1, τ_2, τ_3 are immediately found to be, respectively,

$$\tfrac{1}{2}(\sigma_2 + \sigma_3) \qquad \tfrac{1}{2}(\sigma_1 + \sigma_3) \qquad \tfrac{1}{2}(\sigma_1 + \sigma_2)$$

In view of the assumption $\sigma_1 > \sigma_2 > \sigma_3$, the greatest shear stress is of magnitude $\frac{1}{2}(\sigma_1 - \sigma_3)$, and it acts across a plane whose normal bisects the angle between the directions of σ_1 and σ_3. It follows from (32) that the greatest shear stress is equal to $\sqrt{J_2}\cos(\pi/6 - \phi)$, where ϕ lies between zero and $\pi/3$ satisfying (31).

(v) ***Shear stress and the oblique triangle*** Consider now the direction of the shear stress on an inclined plane in relation to the true shape of the oblique triangle. It is assumed for simplicity that the direction cosines (l, m, n) are all positive.† Let δh denote the perpendicular distance from the origin O to the oblique plane ABC (Fig. 1.10*a*). Then the distances of the vertices A, B, C from O are $\delta h/l$, $\delta h/m$, $\delta h/n$ respectively, their ratios being

$$OA{:}OB{:}OC = mn{:}nl{:}lm \tag{38}$$

The sides of the triangle are readily found from the right-angled triangles AOB, BOC, and COA. The true shape of the oblique triangle ABC is therefore defined by the ratios

$$AB{:}BC{:}CA = n\sqrt{1-n^2}{:}l\sqrt{1-l^2}{:}m\sqrt{1-m^2} \tag{39}$$

† No generality is lost in this assumption, since the positive directions of the axes of reference can be arbitrarily chosen, and the expressions for σ and τ involve only the squares of the direction cosines.

The vertical angles of the triangle follow from (39) and the well-known cosine law. The results can be conveniently put in the form

$$\tan A = \frac{l}{mn} \qquad \tan B = \frac{m}{nl} \qquad \tan C = \frac{n}{lm} \tag{40}$$

The coordinate axes in Fig. 1.10*a* are in the directions of the principal stresses. A line *BD* is drawn from the apex *B* to meet the opposite side of *AC* at *D*, such that *BD* is perpendicular to the direction of the shear stress across the plane. The components of the vector **BD** along the axes *Ox*, *Oy*, *Oz* are equal to *ED*, –*OB*, *OE* respectively. Since *BD* is orthogonal to both the directions (l, m, n) and (l_s, m_s, n_s), the scalar products of **BD** with the unit vectors representing these directions must vanish. Using (35) and (33), it is easily shown that

$$ED{:}OB{:}OE = mn(\sigma_2 - \sigma_3){:}nl(\sigma_1 - \sigma_3){:}lm(\sigma_1 - \sigma_2) \tag{41}$$

If $\sigma_1 > \sigma_2 > \sigma_3$, the line *BD* must meet *AC* internally as shown. Indeed, from the similar triangles *CDE* and *CAO*, we have

$$\frac{CD}{CA} = \frac{ED}{OA} = \frac{ED}{OB}\frac{OB}{OA} = \frac{\sigma_2 - \sigma_3}{\sigma_1 - \sigma_3} \tag{42}$$

in view of (38) and (41). If points *A*, *D*, *C*, and *G* are located along a straight line, such that $GA = \sigma_1$, $GD = \sigma_2$, and $GC = \sigma_3$, and the true shape triangle *ABC* is constructed on *CA* as base (Fig. 1.10*b*), then in view of (42), the shear stress is directed at right angles to the line joining *B* and *D*. Since $n_s < 0$ by (35), the direction of the shear stress vector is obtained by a 90° counterclockwise rotation from the direction *BD*. If *R* is the orthocenter of the triangle *ABC*, and *BM* is drawn perpendicular to *CA*, then by Eqs. (40),

$$\frac{CM}{AM} = \frac{\cot C}{\cot A} = \frac{l^2}{n^2} \qquad \frac{MR}{MB} = \frac{\cot A}{\tan C} = m^2 \tag{43}$$

since angle *MRC* is equal to the vertical angle *A*. If *RN* is drawn parallel to *BD*, meeting *CA* at *N*, then $MN/MD = MR/MB = m^2$, which gives

$$\begin{aligned} GN &= GM + MN = (l^2 + m^2 + n^2)GM + m^2 MD \\ &= l^2(GA - MA) + m^2 GD + n^2(GC + CM) = l^2 GA + m^2 GD + n^2 GC \end{aligned}$$

The expression on the right-hand side is equal to σ in view of (33). Hence *GN* represents the magnitude of the normal stress transmitted across the plane.† It follows from (34) and (41) that if *OB* represents the quantity $nl(\sigma_1 - \sigma_3)$ to a certain scale, then *BD* will represent the shear stress τ to the same scale. Hence

$$\frac{OB}{BD} = nl\left(\frac{\sigma_1 - \sigma_3}{\tau}\right) = \frac{nl}{\tau}CA$$

† The constructions for the normal stress and the direction of the shear stress are due to H. W. Swift, *Engineering*, **162**: 381 (1946).

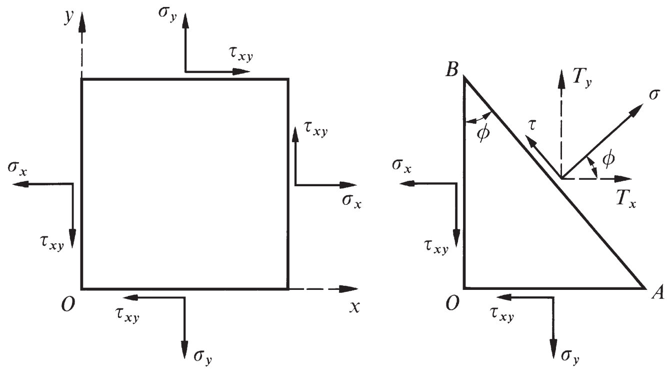

Figure 1.11 An element in a state of plane stress.

with reference to Fig. 1.10. Since $RN/BD = MR/MB = m^2$ by (43), and $CA = \sqrt{OC^2 + OA^2}$, we have

$$RN = m^2 \cdot BD = \frac{m^2\tau}{nl}\frac{OB}{CA} = \frac{m\tau}{\sqrt{1-m^2}}$$

in view of (38). It follows that the magnitude of the shear stress on the plane is $\tau = RN \tan\beta$, where β is the angle made by the normal to the plane with the direction of the intermediate principal stress σ_2.

(vi) ***Plane stress*** A state of plane stress is defined by $\sigma_z = \tau_{yz} = \tau_{zx} = 0$. The z axis then coincides with a principal axis, and the corresponding principal stress vanishes.† The orientation of Ox and Oy with respect to the other two principal axes is, however, arbitrary. Consider a plane AB perpendicular to the xy plane, and let ϕ be the counterclockwise angle made by the normal to the plane with the x axis (Fig. 1.11). The shear stress τ will be reckoned positive when it is directed to the left of the exterior normal. Setting $l = \cos\phi$, $m = \sin\phi$, and $n = 0$ in (16), the components of the stress vector across AB are obtained as

$$T_x = \sigma_x \cos\phi + \tau_{xy}\sin\phi \qquad T_y = \tau_{xy}\cos\phi + \sigma_y \sin\phi \tag{44}$$

The resolved components of the resultant stress along the normal and the tangent to the plane are

$$\sigma = T_x\cos\phi + T_y\sin\phi \qquad \tau = -T_x\sin\phi + T_y\cos\phi$$

† The results for plane stress are directly applicable to the more general situation where the z axis coincides with the direction of any nonzero principal stress.

Substituting for T_x and T_y in the above equations, the normal and shear stresses across the plane are obtained as

$$\begin{aligned}\sigma &= \sigma_x \cos^2\phi + \sigma_y \sin^2\phi + 2\tau_{xy} \sin\phi \cos\phi \\ &= \tfrac{1}{2}(\sigma_x + \sigma_y) + \tfrac{1}{2}(\sigma_x - \sigma_y)\cos 2\phi + \tau_{xy} \sin 2\phi \qquad (45)\\ \tau &= -(\sigma_x - \sigma_y)\sin\phi\cos\phi + \tau_{xy}(\cos^2\phi - \sin^2\phi) \\ &= -\tfrac{1}{2}(\sigma_x - \sigma_y)\sin 2\phi + \tau_{xy}\cos 2\phi \qquad (46)\end{aligned}$$

These results may be directly obtained from (16) and (17) by setting $l = m' = \cos\phi$, $m = -l' = \sin\phi$ and $n = n' = 0$. Since $d\sigma/d\phi = 2\tau$, which is readily verified from above, the shear stress vanishes on the plane for which the normal stress has a stationary value. This corresponds to $\phi = \alpha$, where

$$\tan 2\alpha = \frac{2\tau_{xy}}{\sigma_x - \sigma_y} \qquad (47)$$

which defines two directions at right angles to one another, giving the principal axes in the plane of Ox and Oy. The principal stresses σ_1, σ_2 are the roots of the equation

$$(\sigma - \sigma_x)(\sigma - \sigma_y) = \tau_{xy}^2$$

which is obtained by writing $T_x = \sigma\cos\phi$ and $T_y = \sigma\sin\phi$ in (44), and then eliminating ϕ between the two equations. The solution is

$$\sigma_1, \sigma_2 = \tfrac{1}{2}(\sigma_x + \sigma_y) \pm \tfrac{1}{2}\sqrt{(\sigma_x - \sigma_y)^2 + 4\tau_{xy}^2} \qquad (48)$$

The acute angle made by the direction of the algebraically greater principal stress σ_1 with the x axis is measured in the counterclockwise sense when τ_{xy} is positive, and in the clockwise sense when τ_{xy} is negative. It follows from (48) that

$$\sigma_x + \sigma_y = \sigma_1 + \sigma_2 \qquad \sigma_x\sigma_y - \tau_{xy}^2 = \sigma_1\sigma_2 \qquad (49)$$

These are the basic invariants of the stress tensor in a state of plane stress. Evidently, any function of these invariants is also an invariant.

Let $O\xi$, and $O\eta$ represent a new pair of rectangular axes in the (x, y) plane, and let ϕ be the angle of inclination of the ξ axis to the x axis measured in the counterclockwise sense. Then the stress components σ_ξ and $\tau_{\xi\eta}$, referred to the new axes, are directly given by the right-hand sides of (45) and (46) respectively. The remaining stress component σ_η is obtained by writing $\pi/2 + \phi$ for ϕ in (45), resulting in

$$\begin{aligned}\sigma_\eta &= \sigma_x \sin^2\phi + \sigma_y \cos^2\phi - 2\tau_{xy}\sin\phi\cos\phi \\ &= \tfrac{1}{2}(\sigma_x + \sigma_y) - \tfrac{1}{2}(\sigma_x - \sigma_y)\cos 2\phi - \tau_{xy}\sin 2\phi \qquad (50)\end{aligned}$$

It immediately follows that $\sigma_\xi + \sigma_\eta = \sigma_x + \sigma_y$, which shows the invariance of the first expression of (49). The invariance of the second expression may be similarly verified.

Considering the principal axes as the axes of reference, the shear stress across an inclined plane can be written as $\tau = -\frac{1}{2}(\sigma_1 - \sigma_2)\sin 2\phi$, which indicates that the shear stress is directed to the right of the outward normal to the plane when $\sigma_1 > \sigma_2$ and $0 < \phi < \pi/2$. The shear stress has its greatest magnitude when $\phi = \pm\pi/4$, the maximum value of the shear stress being

$$\tau_{\max} = \frac{1}{2}|\sigma_1 - \sigma_2| = \frac{1}{2}\sqrt{(\sigma_x - \sigma_y)^2 + 4\tau_{xy}^2} \tag{51}$$

There are two other principal shear stresses, having magnitudes $\frac{1}{2}|\sigma_1|$ and $\frac{1}{2}|\sigma_2|$, and bisecting the angles between the z axis and the directions of σ_1 and σ_2 respectively. A little examination of the three principal values reveals that the numerically greatest shear stress occurs in the plane of the applied stresses when σ_1 and σ_2 have opposite signs, and out of the plane of the applied stresses when they are of the same sign. In view of (49), the former corresponds to $\sigma_x\sigma_y < \tau_{xy}^2$ and the latter to $\sigma_x\sigma_y > \tau_{xy}^2$. A state of pure shear is given by $\sigma_1 = -\sigma_2$, since the normal stress then vanishes on the planes of maximum shear.

1.4 Mohr's Representation of Stress

(i) ***Two-dimensional stress state*** A useful graphical method of analyzing the state of stress has been developed by Mohr.† In this method, the normal and shear stresses across any plane are represented by a point on a plane diagram in which σ and τ are taken as rectangular coordinates. For the present purpose, it is necessary to regard the shear stress as positive when it has a clockwise moment about a point within the element. In Fig. 1.12, the stresses acting on planes perpendicular to the x and y axes are represented by the points X and Y on the (σ, τ) plane. The circle drawn on XY as diameter, and having its center C on the σ axis, is called the Mohr circle for the considered state of stress. The points A and B, where the circle is intersected by the σ axis, define the principal stresses, since $OA = \sigma_1$ and $OB = \sigma_2$ in view of (48) and the geometry of Mohr's diagram. By (47), the angle made by CA with CX is twice the angle α which the direction of σ_1 makes with the x axis in the physical plane. The normal and shear stresses transmitted across a plane, whose normal is inclined at a counterclockwise angle ϕ to the x axis, correspond to the point L on the Mohr circle, where CL is inclined to CX at an angle 2ϕ measured in the same sense. The proof of the construction follows from the fact that $CD = CL\cos 2\alpha$ and $XD = CL$ $\sin 2\alpha$, where XD is perpendicular to OA. Then from the geometry of the figure,

$$ON = OC + CL\cos 2(\alpha - \phi) = OC + CD\cos 2\phi + XD\sin 2\phi$$

$$LN = CL\sin 2(\alpha - \phi) = -CD\sin 2\phi + XD\cos 2\phi$$

These expressions are equivalent to (45) and (46) in view of the present sign convention. If LC is produced to meet the circle again at M, then the coordinates of M give

† O. Mohr, *Zivilingenieur*, **28**: 112 (1882). See also his book, *Technische Mechanik*, Berlin (1906).

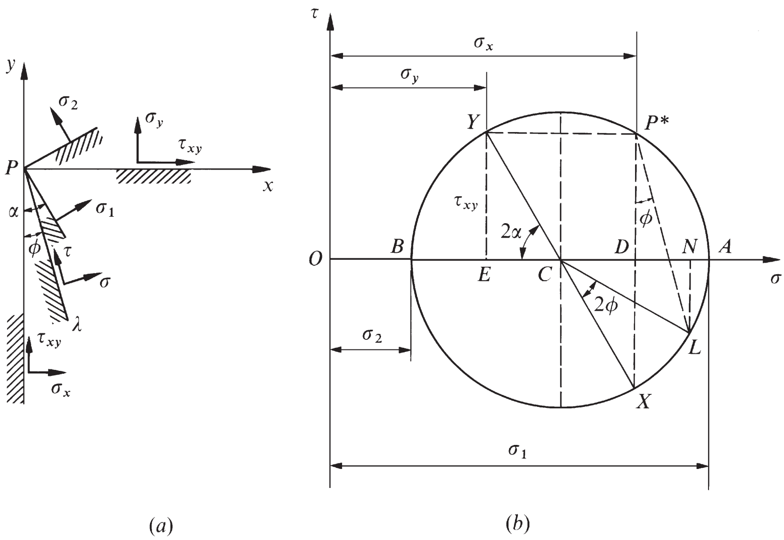

Figure 1.12 Mohr's construction for a two-dimensional state of stress. (*a*) Physical plane; (*b*) stress plane.

the stresses across a plane perpendicular to that corresponding to *L*. The maximum shear stress is evidently equal to the radius of the Mohr circle, and acts on planes that correspond to the extremities of the vertical diameter. The normal stress across these planes is equal to the distance of the center of the circle from the origin of the stress plane.

It is instructive to consider the following alternative construction, also due to Mohr. Let a generic point *P*, the state of stress at which is being discussed, be taken as the origin of coordinates in the physical plane (Fig. 1.12*a*). All planes passing through *P* and containing the *z* axis are denoted by their traces in the *xy* plane. The normal and shear stresses corresponding to the points *X* and *Y* on the Mohr circle are transmitted across the planes *Py* and *Px* respectively. The lines through *X* and *Y* drawn parallel to these planes intersect the circle at a common point *P**, which is called the pole of the Mohr circle. When the stress circle and the pole are given, the stresses acting across any plane *P*λ through *P* are found by locating the point *L* on the circle such that *P***L* is parallel to *P*λ, the angle *XCL* at the center being twice the peripheral angle *XP***L* over the arc *XL*. The planes corresponding to the principal stresses are parallel to *P***A* and *P***B*, and those corresponding to the maximum shear stress are parallel to *P***S* and *P***T*. It may be noted that the magnitude of the resultant stress across any plane is equal to the distance of the corresponding stress point on the Mohr circle from the origin of the stress plane.

(ii) ***Three-dimensional stress state*** Suppose that the principal stresses σ_1, σ_2, σ_3 are known in magnitude and direction for a three-dimensional state of stress. These principal values are assumed as distinct, and so labeled that $\sigma_1 > \sigma_2 > \sigma_3$. A graphical method developed by Mohr can be used to find the variation of normal and shear stresses with the direction (l, m, n). We begin with the relations

$$\begin{aligned} l^2\sigma_1 + m^2\sigma_2 + n^2\sigma_3 &= \sigma \\ l^2\sigma_1^2 + m^2\sigma_2^2 + n^2\sigma_3^2 &= \sigma^2 + \tau^2 \\ l^2 + m^2 + n^2 &= 1 \end{aligned} \tag{52}$$

This is a set of three linear equations for the squares of the direction cosines. The solution is most conveniently obtained by eliminating n^2 from the first two equations by means of the third, resulting in

$$l^2 = \frac{(\sigma - \sigma_2)(\sigma - \sigma_3) + \tau^2}{(\sigma_1 - \sigma_2)(\sigma_1 - \sigma_3)} \tag{53}$$

$$m^2 = \frac{(\sigma - \sigma_3)(\sigma - \sigma_1) + \tau^2}{(\sigma_2 - \sigma_3)(\sigma_2 - \sigma_1)} \tag{54}$$

$$n^2 = \frac{(\sigma - \sigma_1)(\sigma - \sigma_2) + \tau^2}{(\sigma_3 - \sigma_1)(\sigma_3 - \sigma_2)} \tag{55}$$

Let one of the direction cosines, say n, be held constant while the other two are varied. By (55), the normal and shear stresses then vary according to the equation

$$\tau^2 + \{\sigma - \tfrac{1}{2}(\sigma_1 + \sigma_2)\}^2 = \tfrac{1}{4}(\sigma_1 - \sigma_2)^2 + n^2(\sigma_1 - \sigma_3)(\sigma_2 - \sigma_3) \tag{56}$$

In the stress plane, σ and τ therefore lie on a circle whose center is on the σ axis at a distance $\frac{1}{2}(\sigma_1 + \sigma_2)$ from the origin. The square of the radius of the circle is given by the right-hand side of (56). The radius varies from $\frac{1}{2}(\sigma_1 - \sigma_2)$ for $n = 0$ to $\frac{1}{2}(\sigma_1 + \sigma_2) - \sigma_3$ for $n = 1$.

In Fig. 1.13, the points A, B, C with coordinates $(\sigma_1, 0)$, $(\sigma_2, 0)$, $(\sigma_3, 0)$ are the principal points of the Mohr diagram. The centers of the segments AB, BC, and CA are denoted by the points P, Q, and R. The upper semicircle drawn on the diameter AB corresponds to $n = 0$. As n increases from 0 to 1, the radius of the semicircle varies from PB to PC. Similarly, the upper semicircles with BC and CA as diameters correspond to $l = 0$ and $m = 0$ respectively. For constant values of l, (53) defines a family of circles having the equation

$$\tau^2 + \{\sigma - \tfrac{1}{2}(\sigma_2 + \sigma_3)\}^2 = \tfrac{1}{4}(\sigma_2 - \sigma_3)^2 + l^2(\sigma_1 - \sigma_2)(\sigma_1 - \sigma_3) \tag{57}$$

The center of these circles is at Q, while the radius varies from QB for $l = 0$ to QA for $l = 1$. Finally, considering constant values of m, we have the family of circles

$$\tau^2 + \{\sigma - \tfrac{1}{2}(\sigma_1 + \sigma_3)\}^2 = \tfrac{1}{4}(\sigma_1 - \sigma_3)^2 + m^2(\sigma_1 - \sigma_2)(\sigma_3 - \sigma_2) \tag{58}$$

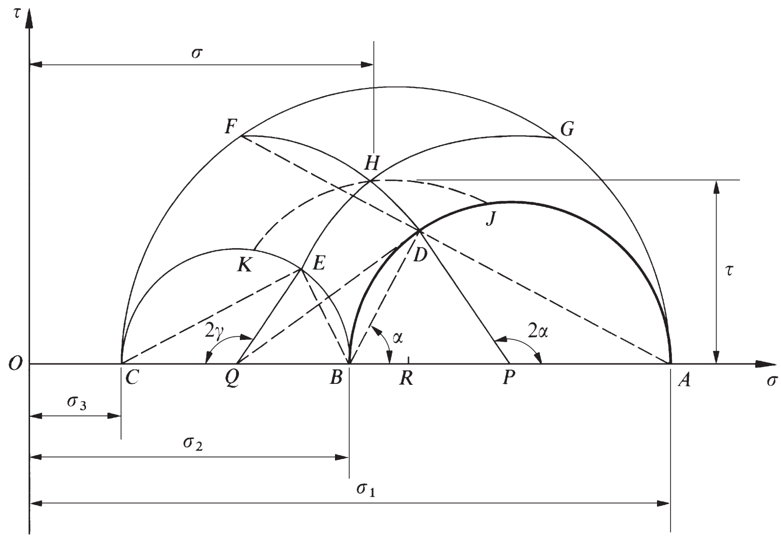

Figure 1.13 Mohr's representation of stress in three dimensions.

with the center at R, and the radius decreasing from RC for $m = 0$ to RB for $m = 1$. For arbitrary values of (l, m, n), the state of stress will correspond to a point in the space between the three semicircles drawn on the diameters AB, BC, and CA.

To find the values of σ and τ across any given plane, let $\alpha = \cos^{-1} l$ and $\gamma = \cos^{-1} n$ be the angles made by the normal to the plane with the directions of σ_1 and σ_3 respectively. Set off angles APD and CQE equal to 2α and 2γ respectively, by drawing the radii PD and QE to the appropriate semicircles. The circular arcs DHF and EHG, drawn with centers Q and P respectively, intersect one another at H giving the required stress point.† If the lines AD and CE are produced, they will meet the outermost semicircle at F and G respectively. Since the angle ABD is equal to α, and $BD = (\sigma_1 - \sigma_2)\cos\alpha$, the triangle BDQ furnishes

$$\begin{aligned} QD^2 &= QB^2 + BD^2 + 2QB \cdot BD \cos\alpha \\ &= \tfrac{1}{4}(\sigma_2 - \sigma_3)^2 + (\sigma_1 - \sigma_2)(\sigma_1 - \sigma_3)\cos^2\alpha \end{aligned}$$

Hence QD is identical to the radius of the circle (57) corresponding to the given value of l. Similarly, the radius PE is equal to that of the circle (56) corresponding to the given value of n. This completes the proof of the construction for the stress point H. It can be shown that the circular arc drawn through H with center at R cuts the semicircles on AB and BC at J and K respectively, where BJ and BK are each inclined at an angle $\beta = \cos^{-1} m$ to the vertical through B.

† Numerical examples have been given by J. M. Alexander, *Strength of Materials*, Chap. 4, Ellis Horwood Limited, Chichester, U.K. (1981).